Quantitative Finance

ISSN: 1469-7688 (Print) 1469-7696 (Online) Journal homepage: www.tandfonline.com/journals/rquf20

Modeling variance risk in financial markets using power-laws: new evidence from the Garman-Klass variance estimator

Masoumeh Fathi & Klaus Grobys

To cite this article: Masoumeh Fathi & Klaus Grobys (07 Aug 2025): Modeling variance risk in financial markets using power-laws: new evidence from the Garman-Klass variance estimator, Quantitative Finance, DOI: 10.1080/14697688.2025.2529485

To link to this article: https://doi.org/10.1080/14697688.2025.2529485

Published online: 07 Aug 2025.

Quantitative Finance, 2025
https://doi.org/10.1080/14697688.2025.2529485

Modeling variance risk in financial markets using power-laws: new evidence from the Garman-Klass variance estimator

MASOUMEH FATHI†* and KLAUS GROBYS†‡**

†Finance Research Group, School of Accounting and Finance, University of Vaasa, Wolffintie 34, Vaasa 65200, Finland
‡Innovation and Entrepreneurship (InnoLab), University of Vaasa, Wolffintie 34, Vaasa 65200, Finland

(*Received 2 January 2025; accepted 26 June 2025*)

This study examines the range-based variance risk of five key financial asset markets—S&P 500, gold, crude oil, the USD/GBP exchange rate, and Bitcoin—using the noise-efficient Garman-Klass variance estimator. Our findings corroborate previous research by demonstrating that range-based asset variances adhere to power-law behavior generating variance behavior that is effectively infinite in practical terms. Furthermore, we provide novel evidence that the widely accepted log-normal model is unequivocally rejected for all range-based asset variances, underscoring its inadequacy in capturing the statistical properties of financial asset variances. A key contribution of this study is the discovery that a power-law function with $\alpha \approx 2.8$ represents a universal law governing the cross-sectional variances of otherwise unrelated asset markets. These findings have significant implications for risk management frameworks that rely on models developed within the mean-variance space, as they highlight the limitations of traditional approaches in assessing and managing financial risks.

Keywords: Garman-Klass estimator; Power-laws; Range-based variance; Second moment; Variance of variance

JEL Classification: C18, G10, G12, G14

1. Introduction

The seminal study by Markowitz (1952) laid the groundwork for portfolio analysis of financial assets, introducing the mean-variance framework as the cornerstone for optimizing portfolios of risky assets. Building on this foundation, Treynor (1962), Sharpe (1964), Lintner (1965), and Mossin (1966) developed the Capital Asset Pricing Model (CAPM), which remains a foundational concept in asset pricing literature. However, empirical failures of the CAPM have inspired the development of various factor models, culminating in what Feng *et al*. (2020) term a 'factor zoo.' Among these, the Fama-French factor models (Fama and French 1992, 1993, 2015, 2017, 2018, 2020) are widely recognized as benchmark models in empirical investigations aimed at addressing CAPM's limitations.

It is well understood that 'true' volatility is unobservable, and the literature offers various proxies to estimate it. These include the sample variance, conditional variance modeled through GARCH or stochastic volatility frameworks, and realized and range-based volatility derived from high-frequency or intraday price data. Range-based estimators, such as those proposed by Parkinson (1980) and Garman and Klass (1980), have been shown to be particularly efficient and robust, especially in the presence of market microstructure noise, and are widely used as nonparametric measures of realized variance (Chou *et al*. 2010).

While these factor models offer an appealing theoretical framework, their reliance on the mean-variance space presents critical challenges if the variance is statistically undefined. In his commentary on Mandelbrot's (1963) 'infinite variance hypothesis,' which profoundly disrupted traditional finance theory, Fama (1963) cautioned that statistical tools assuming finite variance—such as least-squares regression—could

*Corresponding author. Email: masoumeh.fathi@uwasa.fi

**Current address: Department of Monetary Economics and International Finance, Christian-Albrechts University (CAU) of Kiel, Wilhelm-Seelig Platz 1, 24118 Kiel, Germany

yield misleading results if variance is infinite. Subsequent evidence suggests that many proposed asset pricing factors may suffer from sample-specificity (Chan *et al*. 2000, Hirshleifer 2001, Schwert 2003). Extending this discourse, Grobys (2021) posited that replication failures in financial economics could stem from infinite variances or infinite variance of variances. Importantly, the qualitative implications of these phenomena are effectively identical.

This study aims to address a fundamental question: does the population mean of range-based variances in financial markets exist? Here, we focus on range-based realized variances, which serve as ex-post estimators of volatility and approximate the latent conditional variance of returns. Unlike model-based residual variance, which reflects unexplained variation after regression and depends on model assumptions, range-based variance is directly observable and model-free. If the distribution of these range-based variances exhibits extremely heavy tails, this implies that variance estimates themselves are unstable and potentially without finite moments. Consequently, the residual variance in linear regression models (e.g. CAPM or Fama-French), which requires the theoretical variance of the inputs to be statistically well-defined, may itself become undefined, thereby invalidating classical inference tools such as standard errors, t-statistics, and R^2. This makes the investigation of tail behavior in, for example, range-based variance distributions essential for assessing the reliability of asset pricing models built on OLS regression.

To this end, we investigate range-based variances in five major financial asset markets—S&P 500, gold, crude oil, the USD/GBP exchange rate, and Bitcoin—using intraday data. Range-based variances are computed using the Garman-Klass range-based variance estimator. We also fit power-law models to the data using maximum likelihood estimation (MLE) to examine the statistical properties of extreme variance realizations, with a specific focus on the tail behavior of the distribution beyond the range of typical observations. To assess model suitability, we conduct comprehensive goodness-of-fit tests, comparing the power-law hypothesis against other plausible distributions, such as log-normal and exponential models. Given the dependency structures in financial variance data (e.g. volatility clustering), we orthogonalize the range-based variance data through autoregressive modeling and reapply goodness-of-fit tests to the resulting innovation processes. Furthermore, we test for commonalities in the range-based variances of unrelated asset markets by examining whether power-law behavior is statistically invariant across these markets. Finally, we conduct an extensive set of robustness checks to validate our findings, including sample-split tests, the use of alternative volatility measures (e.g. realized variance), the examination of additional asset classes (e.g. bonds), the application of Bayesian inference to estimate tail exponents and cutoffs, model comparisons using Akaike Information Criterion (AIC) alongside the Kolmogorov–Smirnov test, rolling-window estimations, and the fitting of tempered stable and Generalized Beta of the Second Kind (GB2) distributions to assess the stability and generality of the observed power-law behavior.

This study makes several significant contributions to the literature, addressing critical methodological, theoretical, and empirical gaps. These contributions advance our understanding of range-based variances in financial markets and their implications for asset pricing and risk management. First, previous research, such as Grobys (2021), relied on the Parkinson variance estimator (Parkinson 1980) to compute range-based variances. While this approach has merits, Molnár (2012) highlighted that range-based variance estimators, such as those proposed by Garman and Klass (1980), outperform alternatives when accounting for noise in high-frequency data. Chou *et al*. (2010) also emphasized the informational advantage of intraday price ranges over closing prices. By adopting the Garman-Klass variance estimator, this study mitigates potential biases inherent in the use of inflated variance estimators, as in the study of Grobys (2021). Our methodological adjustment ensures greater precision in capturing range-based variances, offering a robust foundation for further analysis. This refinement is essential to derive reliable insights, particularly when assessing heavy-tailed distributions like power laws, and aligns with calls from Molnár (2012) for a more rigorous treatment of variance estimation methods.

Second, realized volatility has long been theorized as log-normal, with Andersen *et al*. (2001) providing seminal empirical support for this assumption. However, evidence challenging this perspective has been mounting. Renó and Rizza (2003), for instance, demonstrated that volatility in Italian futures markets aligns more closely with a Pareto distribution, necessitating the rejection of log-normality. Fathi *et al*. (2024) further confirmed power law distributions as superior in capturing realized variances in G10 currencies. Our study expands on this work by rigorously comparing the log-normal, exponential, and power-law models using comprehensive goodness-of-fit tests. We provide robust evidence that power laws offer the most plausible framework for modeling daily range-based variances too. By reconciling theoretical assumptions with observed data, this study extends Grobys' (2021) findings, which focused exclusively on power-law validity.

Third, Grobys (2021) used a relatively narrow sample, such as range-based variances for gold from August 30, 2000, to March 31, 2021, missing critical periods such as the gold price bubbles of the 1980s. Data omissions of this nature can lead to upward-biased estimates of power-law exponents, particularly if extreme events are underrepresented. To address this limitation, we extend the dataset for gold to cover February 7, 1980, to July 31, 2024, more than doubling the observation count to 11 196. This comprehensive data expansion ensures that periods of significant market stress are incorporated, mitigating biases and strengthening the reliability of our findings. By filling this empirical gap, the study builds a robust foundation for analyzing power-law behavior of range-based asset market variances.

Fourth, studies have explored common power-law behavior of range-based variances within related asset categories, such as equity factors (Fathi *et al*. 2025) and foreign exchange markets (Grobys 2024). These works documented universal exponents (e.g. $\alpha \approx 2.6$ for range-based variances of G10 currencies) that imply risk homogeneity within specific asset classes. However, no prior research has tested for such commonality across unrelated markets. This study pioneers cross-sectional risk analysis by examining whether the range-based variances

of diverse financial markets, including equities, commodities, exchange rates, and cryptocurrencies are governed by a common power law. The existence of such a commonality would suggest a shared underlying risk dynamic, likely driven by similar systemic or behavioral forces, such as herding behavior. The identification of a cross-market universal exponent would underscore the need for unified risk modeling approaches and contributes a novel dimension to the literature on power-law behavior.

Finally, robustness is a critical aspect of econometric analysis, especially when dealing with heavy-tailed distributions. Unlike Grobys (2021), which relied primarily on raw data, we employ autoregressive modeling to account for volatility clustering, a well-documented phenomenon in financial markets. Analyzing the resulting innovation processes confirms that power-law behavior persists even after accounting for dynamic dependencies. Furthermore, our sample-split tests validate the stability of power-law exponents across time periods and subsamples. These methodological advancements align with calls for more robust analytical frameworks in the financial econometrics literature (Mandelbrot 1963, Grobys 2021, Fathi *et al*. 2024) and enhance the generalizability of our findings.

Through these contributions, the study directly engages with and builds upon prior literature, addressing gaps in methodologies (Molnár 2012), theoretical assumptions (Andersen *et al*. 2001, Renó and Rizza 2003), and empirical scope (Grobys 2021, Fathi *et al*. 2024). By leveraging improved variance estimators, expanding datasets, and incorporating cross-sectional and dynamic robustness analyses, the research advances our understanding of range-based variances across financial markets. It also underscores the limitations of traditional models, advocating for the integration of power-law frameworks to better capture the realities of extreme market risks. These findings hold critical implications for both academic research and practical applications in risk management, portfolio optimization, and asset pricing.

The results reveal that Garman-Klass range-based variances exhibit heavy tails across all five markets, strongly supporting the power-law hypothesis. The MLE analysis of tail exponents confirms that values consistently fall within $2 < \alpha < 3$, implying infinite variance. This corroborates earlier findings (e.g. Grobys 2021, 2024, Fathi *et al*. 2024, 2025) and raises critical concerns about traditional econometric techniques relying on finite-variance assumptions. Goodness-of-fit tests firmly reject alternative distributions, including log-normal and exponential models, highlighting the systematic underestimation of tail risks by finite-moment frameworks. Moreover, striking evidence supports the existence of a universal cross-sectional power-law exponent ($\alpha \approx 2.8$) governing range-based variances across unrelated markets. Robustness checks using autoregressive modeling and sample-split tests confirm these findings, underscoring their consistency across time periods and market conditions.

This study provides critical insights into the statistical properties of range-based variances across key financial markets, offering important implications for finance theory and practice. First, the evidence of practically infinite variance challenges traditional econometric methods, such as point estimation and hypothesis testing, which assume finite variance, necessitating the development of alternative methodologies. Second, the rejection of the log-normal model in favor of power-law distributions highlights the systematic underestimation of tail risks by finite-moment frameworks, emphasizing the need for power-law-based approaches in assessing and managing extreme financial risks. Third, the identification of a universal power-law exponent across unrelated markets implies limited diversification benefits, as common dynamics across asset variances may amplify systemic risks, urging the adoption of unified risk modeling strategies. Fourth, the robustness of power-law exponents across time periods and subsamples, even after accounting for volatility clustering, confirms the generality and consistency of these findings, supporting their applicability to a wide range of financial contexts. Collectively, these results challenge prevailing assumptions underpinning modern portfolio theory and traditional risk management frameworks, reinforcing the necessity for alternative approaches that better capture the realities of extreme financial risks. By addressing methodological, theoretical, and empirical gaps, this study paves the way for more accurate risk modeling, portfolio optimization, and the development of financial instruments resilient to market extremes.

This study is organized as follows: Section 2 reviews the relevant literature; Section 3 describes the data; Section 4 outlines the methodology; Section 5 presents the empirical results and key findings; Section 6 discusses their implications; and Section 7 concludes the study.

2. Literature review

The modeling of volatility in financial markets has evolved into a rich and multifaceted area of research, resulting in a variety of theoretical and empirical frameworks. These models are designed to capture different aspects of volatility behavior, ranging from short-term clustering to long-memory and heavy-tailed properties. This literature can be grouped into six major research streams: GARCH-type models, stochastic volatility models, realized volatility models, range-based volatility models, multifractal and scaling models, and power-law (namely, tail-index) approaches.

2.1. Generalized Autoregressive Conditional Heteroskedasticity (GARCH) models

The Generalized Autoregressive Conditional Heteroskedasticity (GARCH) model, introduced by Bollerslev (1986), and its variants have become foundational in volatility modeling. These models describe volatility as a conditional process that evolves based on past squared returns and past variances. Key extensions include the Exponential GARCH (EGARCH) model by Nelson (1991) and the Threshold GARCH (TGARCH) model by Zakoian (1994), which allow for asymmetry in volatility responses. Although highly flexible, these models rely on parametric assumptions and are typically calibrated on daily or lower-frequency data. They perform well in capturing volatility clustering but struggle with representing extreme tail behavior unless augmented

with fat-tailed distributions for example, Student's t (Hansen 1994). A key limitation of GARCH-type models is that their parameter estimates can change substantially when underlying distributional assumptions are relaxed—for example, when the innovation process is altered from a normal to a Student's t distribution, or vice versa. In this regard, Mandelbrot (2008) criticized the tendency of researchers to 'fix' GARCH models when they failed to perform adequately, instead of abandoning them altogether.

2.2. Stochastic volatility (SV) models

In contrast to GARCH models, stochastic volatility (SV) models treat volatility as a latent stochastic process, independent from return innovations (Taylor 1982, Shephard 2005). These models provide greater flexibility in capturing volatility persistence and allow for richer dynamic structures. Recent developments include score-driven SV models (Creal *et al*. 2013, Harvey and Palumbo 2019), which use the score of the conditional likelihood to update latent volatility components. SV models are often computationally intensive but can better accommodate long-memory and structural breaks.

2.3. Realized volatility models

Realized volatility (RV) models utilize high-frequency intraday returns to construct ex-post volatility measures, offering a data-driven alternative to conditionally specified models. Andersen *et al*. (2001) played a pioneering role by formalizing the concept of realized volatility using the sum of squared intraday returns. This approach avoids strong distributional assumptions and allows researchers to observe and model actual volatility over fixed intervals, for example, daily or weekly periods. Subsequent studies have expanded upon this framework to examine properties for example, the distributional characteristics of RV (Barndorff-Nielsen and Shephard 2002), the impact of microstructure noise and asynchronous trading (Zhang *et al*. 2005), and the decomposition of volatility into continuous and jump components (Barndorff-Nielsen and Shephard 2004). Realized volatility is now a central tool in empirical finance, particularly in measuring and forecasting short-term volatility with high precision.

2.4. Range-based volatility models

Range-based models use daily high, low, open, and close prices to construct volatility estimators. The Parkinson (1980) and Garman and Klass (1980) estimators are seminal examples. These methods are shown to be more efficient than squared return-based measures, especially in the presence of microstructure noise and thin trading. Molnár (2012) and Chou *et al*. (2010) further highlight the robustness of range-based estimators, making them suitable for low-frequency but high-accuracy volatility measurement.

2.5. Multifractal and scaling models

Multifractal models attempt to capture the self-similar, long-memory, and scaling properties observed in financial volatility. The Markov-Switching Multifractal (MSM) model developed by Calvet and Fisher (2004) models volatility as a product of volatility components switching between different regimes at multiple frequencies. Earlier work by Mandelbrot *et al*. (1997) and Müller *et al*. (1997) emphasizes the hierarchical and fractal nature of market volatility, linking it to turbulence-like behavior in financial time series.

2.6. Power-law and tail-index approaches

A distinct stream focuses on the tail behavior of the volatility distribution. Rather than modeling conditional volatility, these approaches examine whether realized volatility or variance follows a power-law distribution with infinite mean or variance. Clauset *et al*. (2009) offer robust tools for tail-index estimation and goodness-of-fit testing. Recent empirical work (e.g. Grobys 2021, 2024) applies these methods to range-based variance data, exploring the implications of heavy-tailed volatility for the validity of classical econometric models for example, OLS regression.

While all these models aim to capture features of financial market volatility, they differ significantly in their assumptions and goals. GARCH and SV models are designed for conditional volatility forecasting, relying on parametric or semi-parametric methods. Realized and range-based models use empirical data to estimate volatility more accurately but often without strong assumptions about underlying distributions. Multifractal models and power-law approaches focus on structural properties like scaling laws and tail behavior. Notably, most traditional models do not explicitly address extremely fat-tailed distributions or long-range dependence in volatility, unless such features are specifically built into the model. The power-law approach is unique in explicitly testing for the existence (or lack) of moments, which has profound implications for econometric modeling and asset pricing.

2.7. Alternative approaches to address heavy tails and long memory in volatility

Notably, the literature on financial volatility offers a range of alternative approaches that contribute to understanding heavy-tailed behavior beyond traditional power-law modeling. For instance, Corsi (2009) introduced the Heterogeneous Autoregressive (HAR) model, which captures long-memory effects in realized volatility by aggregating volatility components across different time horizons. This approach has proven effective in modeling the persistent nature of volatility without requiring high-frequency data. Similarly, Harvey and Palumbo (2019) proposed a score-driven model for realized volatility that dynamically adapts to changes in the underlying data-generating process using a state-space framework. These methods highlight the growing emphasis on flexible and robust volatility modeling frameworks. Furthermore, Barndorff-Nielsen and Shephard (2002) introduced stochastic volatility models driven by Lévy processes, allowing for jumps and capturing the non-Gaussian nature of returns. Similarly, Müller *et al*. (1997) proposed a time-deformation model using multiplicative cascades, revealing scaling laws and volatility components at different frequencies. Engle and

Rangel (2008) addressed long-term volatility trends through a spline-GARCH model that combines smooth structural components with short-term GARCH effects. Calvet and Fisher (2004) developed the MSM model, which generates multifractal volatility patterns and long memory via regime-switching cascades. Bollerslev and Todorov (2011) emphasized jump-tail risk by integrating extreme events into asset price and volatility dynamics, accounting for the role of rare but impactful shocks.

Collectively, these models offer alternative perspectives on how volatility evolves over time under non-Gaussian conditions, and they share common objectives: capturing fat-tailed returns, long-range dependence, volatility clustering, and asymmetric responses to market shocks. While traditional GARCH-type models, including their extensions, are typically parametric and rely on specific distributional assumptions, several of the above frameworks (for example, MSM and multiplicative cascades) adopt semi- or non-parametric approaches, allowing for greater flexibility in capturing the empirical irregularities of financial time series. Moreover, models based on realized measures, for example, range-based or high-frequency volatility, circumvent strong distributional assumptions by leveraging more granular data. We have now referenced these studies in the revised manuscript to better position our research within this broader academic discourse and to clarify how our focus on power-law behavior and extreme variance dynamics complements, instead of contradicts, the insights offered by these alternative models.

While the existing literature offers valuable insights into the dynamics and persistence of volatility, our study diverges by explicitly focusing on the tail behavior of the volatility distribution—measured in terms of range-based variances—itself. Rather than modeling the full distribution or volatility path, this study investigates whether the extreme realizations of the data generating process—often dismissed as noise—may actually be governed by a power-law distribution, suggesting that the tail, instead of the center, contains the meaningful signal. This tail-centric perspective enables us to characterize the statistical properties of extreme variance events, a topic that remains underexplored in much of the existing volatility modeling literature.

3. Data

The data for this study were collected from Yahoo Finance. We retrieved daily observations including open, high, low, and closing prices on S&P 500, gold, crude oil, USD/GBP exchange rate, and Bitcoin. Due to data availability, the data sample for the S&P 500 spans from February 19, 1980, to July 31, 2024, providing 11 207 observations. This extensive period captures over four decades of market activity, including significant events such as the 1987 market crash, the dot-com bubble, the 2008 financial crisis, and the COVID-19 pandemic. For gold, the dataset covers a similarly long timeframe, from February 7, 1980, to July 31, 2024, resulting in 11 196 observations. This period reflects both periods of stability and heightened volatility, such as 2008 financial crisis. The crude oil dataset begins on January 2, 1991, and runs until July 31, 2024, including 8556 observations. Specifically, in our study we use data on West Texas Intermediate (WTI) which is one of the main global benchmark prices for crude oil. This period includes major fluctuations crude oil prices due to events such as the Gulf War, the shale revolution, and the COVID-19-related demand shock. The USD/GBP exchange rate data is available from July 25, 2000, to July 31, 2024, yielding 6263 observations. This timeframe captures significant currency market events, including the global financial crisis and Brexit. Finally, Bitcoin data is available from September 17, 2014, to July 31, 2024, with 3603 observations. This relatively short period reflects the cryptocurrency's promising stage and its rapid growth as a speculative and alternative asset, marked by extreme volatility.

To compute the Garman-Klass variance estimator, which combines open and close prices along with daily highs and lows, we follow the methodology proposed by Garman and Klass (1980) and compute daily range-based variances as:

$$\hat{\sigma}^2_{GK} = 0.5\left[\ln\left(\frac{H_t}{L_t}\right)\right]^2 - [2ln2 - 1]\left[\ln\left(\frac{C_t}{O_t}\right)\right]^2, \quad (1)$$

where H represents the daily high price, L denotes the daily low price, O is the daily opening price, and C refers the daily closing price of each financial asset.

GARCH models typically estimate conditional variances based on closing prices and thus may fail to fully capture the intraday dynamics of price movements (e.g. Andersen *et al*. 2003, 2004, Bubák *et al*. 2011). In contrast, range-based variances—particularly those derived from range-based estimators such as the Garman-Klass method—leverage intraday data (high, low, open, and close prices) to provide a more efficient and information-rich measure of daily volatility. As shown by Garman and Klass (1980) and reinforced by Molnár (2012), range-based estimators outperform return-based estimators, especially in the presence of microstructure noise and market frictions. Given our focus on modeling tail behavior and extreme variance risk, range-based variances offer clear advantages: they better capture the heavy-tailed nature of financial markets and are less prone to distributional misspecification. This allows for a more robust empirical foundation when testing power-law behavior and modeling the variance of variance—a key objective of our study.

Table 1 reports the descriptive statistics for the annualized daily range-based variances of these assets. The statistics show significant variations in the mean, standard deviation, skewness, and kurtosis, indicating the existence of heavy tails in the distribution of range-based variances, which could indicate power-law behavior. The mean of Garman-Klass range-based variance ranges from 0.95 for the USD/GBP exchange rate to 36.18 for Bitcoin, indicating substantial variation in the average level of volatility. Bitcoin's high Garman-Klass range-based variance mean value reflects its nature as a speculative and emergent asset class, characterized by extreme price fluctuations. Similarly, crude oil exhibits a high mean variance of 14.46. Conversely, traditional asset classes like gold (2.79) and the S&P 500 (2.18) show relatively moderate average variances, aligning with their roles as more stable investment assets. The USD/GBP exchange rate, with a

mean of 0.95, suggests that currency markets involving major economies tend to exhibit lower volatility. In addition, all assets exhibit significant positive skewness and excess kurtosis, suggesting non-normality in their range-based variance distributions. Crude oil exhibits the highest skewness and kurtosis (skewness: 88.83, kurtosis: 8095.44), while Bitcoin has the lowest skewness and kurtosis (skewness: 9.50, kurtosis: 130.54) among the analyzed assets.

4. Methodology

4.1. Main analysis

4.1.1. Estimating power-law exponents via MLE and comparing model fit. Following earlier studies (Grobys 2021, 2023, 2024, Fathi *et al*. 2024, 2025), we model the Garman-Klass range-based variances of each asset in our sample using a power-law function, expressed as:

$$p(x) = Cx^{-\alpha}, \tag{2}$$

where $C = (\alpha - 1)x_{MIN}^{\alpha-1}$ with $\alpha \in \{\mathbb{R}_+ | \alpha > 1\}$, and $x = \sigma_{j,t}^2$ denotes the respective range-based Garman-Klass variance of financial asset j at time t. Note that $x \in \{\mathbb{R}_+ | x_{MIN} \leq x < \infty\}$, where x_{MIN} is the minimum threshold for variance values governed by the power-law distribution, and α represents the tail exponent.

For range-based variances exceeding x_{MIN} $(X > x_{MIN})$, the conditional expected first moment is defined as:

$$E[X|X > x_{MIN}] = \int_{x_{MIN}}^{\infty} xp(x)dx = \frac{(\alpha - 1)}{(\alpha - 2)} x_{MIN}. \tag{3}$$

The conditional expected second moment, or the variance of range-based variances for $X > x_{MIN}$, is expressed as:

$$E[X^2|X > x_{MIN}] = \int_{x_{MIN}}^{\infty} x^2 p(x)dx = \frac{(\alpha - 1)}{(\alpha - 3)} x_{MIN}^2. \tag{4}$$

Consequently, higher conditional expected moments of order k follow the general form:

$$E[X^k|X > x_{MIN}] = \frac{(\alpha - 1)}{(\alpha - 1 - k)} x_{MIN}^k. \tag{5}$$

From Equations (3) and (4), it can be concluded that the theoretical mean of range-based Garman-Klass variances is defined only when $\alpha > 2$, while the existence of the variance for range-based Garman-Klass variances requires $\alpha > 3$.

Next, as suggested by White *et al*. (2008) and Clauset *et al*. (2009), we utilized MLE to estimate the power-law tail exponents. The MLE estimator is given by:

$$\hat{\alpha} = 1 + N \left(\sum_{i=1}^{N} \ln \left(\frac{x_i}{x_{MIN}} \right) \right)^{-1}, \tag{6}$$

where $\hat{\alpha}$ is the estimated tail exponent, N is the number of observations exceeding x_{MIN}, and other terms maintain their previously defined meanings. The selection of x_{MIN} is determined by minimizing the distance between the empirical data and the power-law model (Clauset *et al*. 2009). This is achieved using the Kolmogorov–Smirnov (KS) distance, D, which measures the maximum difference between the cumulative distribution functions (CDFs) of the observed data and the fitted model. The distance D is given by:

$$D = MAX_{x \geq x_{MIN}} |S(x) - P(x)|, \tag{7}$$

where $S(x)$ represents the CDF of the empirical data for observations $x \geq x_{MIN}$, and $P(x)$ is the CDF of the fitted power-law model. The optimalx_{MIN} is the value that minimizes D. Additionally, as described by Clauset *et al*. (2009), the standard deviation of the estimated power-law exponents is expressed as:

$$\sigma = \frac{\hat{\alpha} - 1}{\sqrt{N}} + O\left(\frac{1}{N}\right). \tag{8}$$

To verify the appropriateness of a power-law fit, we conducted a goodness-of-fit test based on the KS distance, D, following the methodology derived in Clauset *et al*. (2009) which compares the empirical data to synthetic data generated from a power-law distribution using specific x_{MIN} and $\hat{\alpha}$ values. The null hypothesis of goodness-of-fit test is that the empirical data and the synthetic data generated from a power-law distribution using the estimated x_{MIN} and $\hat{\alpha}$ values belong to the same distribution, suggesting the power-law model is a plausible fit. While the alternative hypothesis suggests that the empirical and synthetic data originate from different distributions, implying that other models should be considered.

Thus, we generated synthetic datasets using the estimated parameters x_{MIN} and $\hat{\alpha}$ in the prior analysis. For each synthetic dataset, the distance (D_S) was calculated and compared to the distance (D) from the original dataset. The p-value for the goodness-of-fit test is defined as the proportion of synthetic datasets where $D_S > D$, denoted as $\#(D_S > D)/K$, where K is the total number of synthetic datasets. A significance level of 5% was applied, meaning the power-law model is not rejected if $\#D_S > D/K > 0.05$. In addition, to ensure robust results, 1000 synthetic datasets were simulated for each financial asset variance.

However, non-rejected power-law null models ascertained by means of Clauset *et al*.'s (2009) goodness-of-fit test do not necessarily mean that power-law distributions are the best fit for the data, as alternative distributions could potentially offer a better match. In addition, as mentioned earlier, prior studies such as Andersen *et al*. (2001), Andersen *et al*. (2001a, 2001b) have suggested that realized volatility often aligns closely with a log-normal distribution. To address this, we compare the power-law distributions with the log-normal distributions for each range-based asset variance to determine the most suitable model for the data. As noted by Clauset *et al*. (2009), comparing p-values of power-law models with those of alternative distributions, such as log-normal or exponential, provides a robust basis for evaluating the appropriateness of the power-law model. Thus, following the methodology of Clauset *et al*. (2009), we use the same goodness-of-fit test approach applied to the power-law distribution for assessing the plausibility of other competing distributions (viz.,

Table 1. Descriptive statistics.

Statistic	S&*P* 500	Gold	Crude oil	USD/GBP	BTC
Mean	2.18	2.79	14.46	0.95	36.18
Median	0.95	1.42	6.91	0.60	13.66
Maximum	161.31	200.71	15901.67	135.29	1809.48
Minimum	0.00	0.00	0.00	0.00	0.00
Std. Dev.	4.81	5.54	174.13	2.32	90.06
Skewness	14.32	11.90	88.83	35.59	9.50
Kurtosis	342.75	265.07	8095.44	1864.48	130.54
Observations	11207	11196	8556	6263	3603
Period (MM/DD/YYYY)	02/19/1980	02/07/1980	01/02/1991	07/25/2000	09/17/2014
	07/31/2024	07/31/2024	07/31/2024	07/31/2024	07/31/2024

Note: This table presents the descriptive statistics of the annualized daily range-based variance for various assets, including the S&*P* 500, gold, crude oil, USD/GBP exchange rate, and Bitcoin. The annualized daily range-based variances for each asset calculated using the Garman-Klass methodology (Garman and Klass 1980). The statistics reported in this table are sample statistics, which summarize empirical properties observed in the data. While our analysis later demonstrates that the variance of variance is theoretically infinite due to heavy tails ($\alpha \in (2,3)$), these sample-based measures remain meaningful for descriptive purposes. They do not imply the existence of finite theoretical moments.

log-normal, exponential). In this case, the null hypothesis assumes that the alternative distribution is a plausible fit for the data.

4.1.2. Assessing robust standard errors and testing for a common power-law component. Motivated by recent research documenting that range-based foreign exchange rate variances are governed by a universal power-law exponent (Grobys 2024), we explore this issue for the range-based variances of our five asset markets. An important difference between Grobys' (2024) study and our research is that the underlying asset markets in our study are otherwise unrelated, whereas foreign exchange rates are not. Therefore, a common power-law exponent governing the range-based variances of otherwise unrelated asset markets would be a surprising finding. To investigate this issue, we employ the test procedure proposed in the study of Grobys (2024).

While the MLE proposed by Clauset *et al.* (2009) remains asymptotically unbiased even under dependent data, the presence of autocorrelation—manifested, for example, through volatility clustering—can lead to an underestimation of standard errors when standard i.i.d. assumptions are applied. This would result in overly narrow confidence intervals and potentially misleading inference. To address this issue, we implement a block bootstrap method, as recommended by Godfrey (2009) and employed by Grobys (2024), which preserves temporal dependencies within blocks. This adjustment produces more realistic, wider standard errors and thereby ensures that hypothesis testing related to tail exponents is appropriately conservative; that is, our block bootstrap approach mitigates the issue of downward-biased standard errors due to serial dependence. Hence, to address this issue, we first estimate robust standard errors for each range-based asset variance. This is achieved by employing the blocks bootstrap methodology, as outlined in the study of Grobys (2024).

Specifically, a block bootstrap procedure is implemented with the block length m, where $E[m] = T^{1/3}$ following the recommendation by Godfrey (2009) for variance estimation. From a given data vector of range-based variances, $\boldsymbol{x}$, blocks of size m are randomly selected, where m follows a geometric distribution, $m \sim GEO(p)$ with an expected value $E[m] = (1-p)/p$. Thus, in the overall data sample, we use $p = 0.0435, p = 0.0434, p = 0.0476, p = 0.0526$ and $p = 0.0625$ for the range-based variances of the S&P 500, gold, crude oil, USD/GBP exchange rate, and Bitcoin, respectively. Using this bootstrap method, blocks drawn from the data vector $\boldsymbol{x}$ have varying lengths. These randomly selected blocks m are then stacked into a new vector $\boldsymbol{x}^b$ as follows:

$$\boldsymbol{x}_i^b = \begin{bmatrix} m_1 \\ m_2 \\ m_3 \\ \vdots \end{bmatrix}. \tag{9}$$

Again, it is important to note that the lengths of the blocks $m_1, m_2, \ldots$ vary. The process continues until the length of the constructed vector $\boldsymbol{x}^b$ exceeds T. Then, we cut off any observations exceeding T, ensuring that the artificial data vector $\boldsymbol{x}^b$ matches the length of the original data vector $\boldsymbol{x}$. By applying this blocks bootstrap, 1000 artificial data vectors $\begin{bmatrix} \boldsymbol{x}^1 & \boldsymbol{x}^2 & \cdots & \boldsymbol{x}^B \end{bmatrix}$, are generated for each given original data vector. Next, the point estimates $\hat{\alpha}$ for each bootstrap data vector $\begin{bmatrix} \boldsymbol{x}^1 & \boldsymbol{x}^2 & \cdots & \boldsymbol{x}^B \end{bmatrix}$, are calculated and stored in a vector $\begin{bmatrix} \hat{\alpha}^1 & \hat{\alpha}^2 & \cdots & \hat{\alpha}^B \end{bmatrix}$ following the method described by Clauset *et al.* (2009). As a final step, the bootstrapped standard error $\hat{\sigma}_{BOOT}$ is calculated from $\begin{bmatrix} \hat{\alpha}^1 & \hat{\alpha}^2 & \cdots & \hat{\alpha}^B \end{bmatrix}$ for each given data vector of range-based asset variances as:

$$\hat{\sigma}_{BOOT} = \sqrt{\frac{1}{B}\sum_{b=1}^{B}\left(\hat{\alpha}^b - \left(\frac{1}{B}\sum_{b=1}^{B}\hat{\alpha}^b\right)\right)^2}. \tag{10}$$

After obtaining the robust standard errors, we can conduct the joint test to examine whether the Garman-Klass range-based variances of different assets share a common component, represented by a common power-law exponent.

Identifying such a shared exponent would suggest a unified risk of these assets. It is worth noting that our bootstrapping method ensures $COV(\hat{\alpha}_i, \hat{\alpha}_j) = 0 \forall i \neq j$. Based on this, the covariance matrix for estimated power law exponents is defined as:

$$\hat{\mathbf{\Sigma}}_{\hat{\boldsymbol{\alpha}}} = \begin{pmatrix} \hat{\sigma}^2_{\hat{\alpha}_{boot},S\&P500} & 0 & 0 & 0 & 0 \\ 0 & \hat{\sigma}^2_{\hat{\alpha}_{boot},Gold} & 0 & 0 & 0 \\ 0 & 0 & \hat{\sigma}^2_{\hat{\alpha}_{boot},Crudeoil} & 0 & 0 \\ 0 & 0 & 0 & \hat{\sigma}^2_{\hat{\alpha}_{boot},USD/GBP} & 0 \\ 0 & 0 & 0 & 0 & \hat{\sigma}^2_{\hat{\alpha}_{boot},BTC} \end{pmatrix}, \tag{11}$$

where, $\hat{\sigma}^2_{\hat{\alpha}_{boot},S\&P500}, \hat{\sigma}^2_{\hat{\alpha}_{boot},Gold}, \hat{\sigma}^2_{\hat{\alpha}_{boot},Crudeoil}$, $\hat{\sigma}^2_{\hat{\alpha}_{boot},USD/GBP}$ and $\hat{\sigma}^2_{\hat{\alpha}_{boot},BTC}$ represent the corresponding bootstrapped variances (viz., $\hat{\sigma}^2_{BOOT}$). Then, consistent with Grobys (2024), we define the test statistic $\hat{\lambda}$ as follows:

$$\hat{\lambda} = (\hat{\boldsymbol{\alpha}} - q\mathbf{1})' \hat{\mathbf{\Sigma}}^{-1}_{\hat{\boldsymbol{\alpha}}} (\hat{\boldsymbol{\alpha}} - q\mathbf{1}), \tag{12}$$

where the covariance matrix $\hat{\mathbf{\Sigma}}_{\hat{\boldsymbol{\alpha}}}$ is 5×5, $\hat{\boldsymbol{\alpha}}$ represents a 5×1 vector of estimated power-law exponents, $\mathbf{1}$ is a 5×1 vector of ones, and q denoted the hypothesized common power-law exponent. The estimated test statistic $\hat{\lambda}$ in Eq. (10) follows a $\chi^2(5)$ distribution under the null hypothesis, with the corresponding critical value at the 5% significance level being $\chi^2_{0.95}(5) = 11.07$. To evaluate whether the Garman-Klass variances of our five asset markets share a common power-law exponent, the test statistic $\hat{\lambda}$ is iteratively computed across the economically significant range of q values, spanning from 1.2 to 3.2 in increments of 0.1. This iterative computation ensures that the analysis may capture the potential existence of a common power-law exponent governing variance risks across the selected assets.

4.2. Additional analysis

4.2.1. Investigating the impact of autocorrelation on tail index estimates in range-based variances. A potential concern could be whether the observed power-law behavior in the Garman-Klass range-based variance distributions of our assets is genuine or a statistical effect resulting from autocorrelation. It is well-recognized that time-varying volatility can create patterns in the tails of return distributions that resemble power-laws. This phenomenon could lead to inaccurate conclusions, as standard statistical techniques for estimating power laws might incorrectly attribute thick tails to a power-law structure when they are actually produced by a combination of exponential-tail distributions rather than an actual power law. This raises the important question as to whether similar issues affect the estimation of power-law behavior in the range-based variances of our assets?

To examine this, we fit autoregressive models of order p to each asset's Garman-Klass range-based variance. The models are defined as:

$$\hat{\sigma}^2_{j,t} = \beta_{0,j} + \beta_{1,j}\hat{\sigma}^2_{j,t-1} + \beta_{2,j}\hat{\sigma}^2_{j,t-2} + \ldots + \beta_{p,j}\hat{\sigma}^2_{j,t-p} + \varepsilon_{j,t}, \tag{13}$$

where $\hat{\sigma}^2_{j,t}$ defines the Garman-Klass range-based variance of asset j at time t, $\varepsilon_{j,t}$, represents the innovation process, and p is the lag-order. The optimal lag order p is determined by analyzing the partial autocorrelation function. This approach is similar to ARCH-type models, where the conditional variance is modeled using the lagged values of range-based variances directly. Next, we use the absolute values of the estimated innovation processes of each asset, $|\hat{\boldsymbol{\varepsilon}}_{S\&P500}|$, $|\hat{\boldsymbol{\varepsilon}}_{Gold}|$, $|\hat{\boldsymbol{\varepsilon}}_{Crudeoil}|$, $|\hat{\boldsymbol{\varepsilon}}_{USD/GBP}|$, $|\hat{\boldsymbol{\varepsilon}}_{BTC}|$, to re-evaluate the power-law exponents for each asset's orthogonalized range-based variance process. Then, we carried out Clauset *et al.*'s (2009) goodness-of-fit test, following the methodology outlined earlier for the absolute values of the innovation processes for each asset variance. This procedure helps to evaluate whether the observed power-law behavior persists after accounting for autocorrelation, providing a robust check on the validity of the power-law model for our range-based variances.

4.2.2. Evaluating the reliability of power-law exponents: evidence from sample-split tests. To further validate the robustness of the observed power-law behavior in the innovation processes of the range-based variances, we perform a sample-split test. We divide the residual series for each asset, obtained from the autoregressive models (viz., $|\hat{\boldsymbol{\varepsilon}}_{S\&P500}|$, $|\hat{\boldsymbol{\varepsilon}}_{Gold}|$, $|\hat{\boldsymbol{\varepsilon}}_{Crudeoil}|$, $|\hat{\boldsymbol{\varepsilon}}_{USD/GBP}|$, $|\hat{\boldsymbol{\varepsilon}}_{BTC}|$), into two non-overlapping subsamples of equal length. By estimating the power-law exponents for the absolute values of the residuals in each subsample separately, we aim to assess the consistency of the power-law characteristics across different sample episodes. This approach allows us to examine whether the power-law behavior persists independently within each subsample, mitigating concerns about potential sample-specificity. Additionally, we applied the goodness-of-fit tests to the absolute values of the residuals in each subsample to evaluate the validity of the power-law model in both cases.

4.2.3. Alternative measures of asset market variance: A realized variance approach. While the main analysis in this paper is based on the Garman-Klass range-based estimator, concerns can be raised about the potential limitations of relying on a single volatility measure. Specifically, it has been noted that different volatility estimators may capture different aspects of return dynamics, and even the most efficient estimators remain noisy approximations of true volatility (Shu and Zhang 2006, Molnár 2012, Będowska-Sójka and Kliber 2021). To address this concern and assess the robustness of our findings, we extend our analysis by computing weekly realized variances based on the sum of squared daily returns over five-day intervals. This return-based volatility measure offers a conventional benchmark and helps assess whether the heavy-tailed behavior observed under the Garman-Klass estimator persists under a different volatility estimation framework. The daily return of asset market i at time t is computed as follows:

$$RET_{i,t} = 100\frac{(P_{i,t+1} - P_{i,t})}{P_{i,t}}, \tag{14}$$

where $P_{i,t}$ denotes the corresponding daily closing price. Next, we compute the weekly realized variance of each five assets as the sum of the squared returns over five business days according to the following Equation:

$$RV_{j,t} = \sigma_{i,j}^2 = \sum_{t \in j} (RET_{i,t})^2, \tag{15}$$

where j indicates the week and $t \in j$ indicates the corresponding trading days in the respective week. We then estimate power-law exponents for the tail behavior of the weekly realized variances of each asset as described in section 4.1.1. Finally, to evaluate the appropriateness of the power-law model relative to alternative specifications, we compare the empirical data with synthetic data generated from power-law, log-normal, and exponential distributions for each realized asset variance to determine the most suitable model for the weekly data as described in section 4.1.2.

4.2.4. Analysis of additional asset classes: evidence from bonds. To test the generalizability of our findings across asset classes, we extend the analysis to U.S. government bond yields. Specifically, we include range-based bond yield variance data for the 2-year, 5-year, and 10-year Treasury yields, computed using the Garman-Klass estimator on daily high, low, open, and close prices. This addition allows us to explore whether power-law behavior is also present in fixed income markets, which are often considered less volatile than equities or cryptocurrencies. Following the methodology outlined in Section 4.1.1, we estimate power-law exponents for each bond series and conduct comparative goodness-of-fit tests using synthetic data from power-law, log-normal, and exponential distributions. This enables a robust evaluation of the tail behavior in bond market volatility.

4.2.5. Alternative estimation of power-law exponents and cutoffs: A Bayesian inference approach. While our main results rely on the widely used Kolmogorov–Smirnov-based method for estimating power-law parameters, one might be concerned that the selection of the threshold x_{min}—a crucial modeling choice—could influence the inferred tail behavior. To address this potential sensitivity and enhance the credibility of our findings, we perform a robustness check using an alternative, Bayesian estimation framework. This approach follows the methodology introduced by Virkar and Clauset (2014) and Grigaityte and Atwal (2019), which allows for the simultaneous estimation of the power-law exponent $\hat{\alpha}$ and the lower-bound threshold x_{min}. Unlike frequentist methods that rely on point estimates and deterministic threshold selection, the Bayesian approach yields posterior distributions for both parameters. Using Markov Chain Monte Carlo (MCMC) sampling, we generate estimates of $\hat{\alpha}$ and x_{min}. This method not only enhances transparency around threshold selection but also enables a more informative inference by incorporating parameter uncertainty. To formally describe the Bayesian approach, we consider a sample of continuous observations $x_1, x_2, \ldots, x_N$, each satisfying $x_i \geq x_{min}$. The continuous power-law distribution is defined by the following probability density function:

$$p(x|\alpha, x_{min}) = \frac{\alpha - 1}{x_{min}} \left(\frac{x}{x_{min}} \right)^{-\alpha}, \text{for } x \geq x_{min}, \alpha > 1. \tag{16}$$

Given N observations above a threshold x_{min}, the likelihood ($\mathcal{L}$) of the data is:

$$\mathcal{L}(\alpha \mid x, x_{min}) = \prod_{i=1}^{N} \frac{\alpha - 1}{x_{min}} \left(\frac{x_i}{x_{min}} \right)^{-\alpha}. \tag{17}$$

Taking the log, the log-likelihood becomes:

$$log\ \mathcal{L}(\alpha \mid x, x_{min}) = Nlog(\alpha - 1) - Nlog x_{min} - \alpha \sum_{i=1}^{N} log \left(\frac{x_i}{x_{min}} \right). \tag{18}$$

To complete the Bayesian model, we specify prior distributions where for the exponent α, we use a weakly informative uniform *prior:*

$$\alpha \sim Uniform(1.01, 5). \tag{19}$$

In addition, for the threshold x_{min}, we assume a discrete uniform prior over a range of candidate values:

$$x_{min} \in \{x^{(1)}, x^{(2)}, \ldots, x^{(k)}\}, P(x_{min}) = \frac{1}{k}, \tag{20}$$

where, $P(x_{min})$ denotes the prior probability assigned to each candidate threshold, reflecting an assumption of equal plausibility before observing the data. In this setting, the joint posterior distribution over α and x_{min} is given by:

$$P(\alpha, x_{min}|x) \propto \mathcal{L}(\alpha|x, x_{min}) \cdot P(\alpha) \cdot P(x_{min}), \tag{21}$$

where $P(\alpha)$ is the prior distribution over the power-law exponent α. Because x_{min} is discrete and α is continuous, we marginalize over the possible values of x_{min} by computing:

(1) The posterior distribution $P(\alpha|x, x_{min})$ for each candidate x_{min}.
(2) The marginal likelihood (also known as the model evidence):

$$\mathcal{Z}(x_{min}) = \int \mathcal{L}(\alpha|x, x_{min}) \cdot P(\alpha) d\alpha. \tag{22}$$

(3) The posterior over x_{min} using Bayes' rule:

$$P(x_{min}|x) = \frac{\mathcal{Z}(x_{min})}{\sum_{k=1}^{K} \mathcal{Z}(x^k)}. \tag{23}$$

The overall posterior for α can be computed as a weighted mixture of posteriors conditioned on each x_{min}, using the posterior probabilities $P(x_{min}, x)$ as weights. Finally, the power-law exponent and threshold are being estimated by performing MCMC sampling for each candidate ${x_{min}}^{(k)}$, compute their marginal likelihoods, derive posterior probabilities for each threshold, and calculate the weighted posterior mean.

4.2.6. An alternative model comparison metric: the Akaike Information Criterion. In addition to the previously reported goodness-of-fit tests based on Clauset *et al*. (2009), we incorporated a formal model comparison framework to strengthen the case for power-law behavior relative to alternative models. Specifically, we compare the power-law, log-normal, and exponential distributions using the AIC. Unlike the standalone goodness-of-fit tests, AIC provides a systematic approach that balances model fit and complexity through the MLE. For each candidate distribution, model parameters are estimated via MLE. The power-law parameters—the scaling exponent $\widehat{\alpha}$ and the lower bound $\hat{x}_{min}$—are determined following Clauset *et al*. (2009). The log-likelihood for each model is computed based on the corresponding probability density function and the AIC is calculated as:

$$AIC = 2k - 2log(\hat{L}), \tag{24}$$

where k represents the number of parameters (with $k = 1$ for the power-law and exponential models, and $k = 2$ for the log-normal model) and $log(\hat{L})$, is the maximum log-likelihood of the fitted model.

4.2.7. Rolling window estimations for retrieving time-Varying power-law exponents. One could argue that financial volatility may be subject to structural changes over time, potentially challenging the validity of our results from the sample-split tests. In this context, implementing rolling window estimations offers a complementary approach to assess the stability of the estimated power-law exponents. To address this issue, we performed rolling window estimations as follows: for each series of range-based variances, we applied a rolling window of 500 observations and estimated the MLE-based power-law exponent as outlined in Section 4.1.1. The window advances in steps of 50 observations, starting from $t = 500$ until $t = T$.

4.2.8. Estimation of tempered stable distributions. A finding of a shared power-law exponent governing all range-based asset variances would represent a significant theoretical insight. While it may be argued that certain financial assets exhibit distinct distributional characteristics—particularly in response to varying market conditions—such evidence would motivate deeper investigation. Therefore, in this robustness check, we assess whether the tempered stable distribution can offer a more nuanced understanding of the common dynamics underlying range-based variances. A tempered stable distribution generalizes classical stable distributions (e.g. Lévy) by introducing exponential tempering to the heavy tails. This modification allows for finite moments while preserving power-law behavior over intermediate ranges. Formally, the tail decays as

$$P(X > x) \sim x^{-\alpha} e^{-\lambda x}, \tag{25}$$

where $\alpha \in (0, 2)$ controls the tail heaviness and $\lambda > 0$ governs the rate of tempering. This construction retains the scaling properties of stable laws while ensuring statistical regularity in the extreme tails. Tempered stable distributions are particularly useful for modeling empirical phenomena that exhibit approximate power-law scaling but experience faster-than-power decay in the tails, as frequently observed in financial, physical, and biological systems. In applications involving multiple datasets that share a common power-law exponent yet display distinct truncation or decay rates, the tempered stable framework provides a coherent modeling strategy. By fixing a common α across data series and allowing data series-specific tempering parameters λ_i, one can jointly capture universal scaling behavior and dataset-specific tail dynamics. This approach is particularly suited for comparative studies or hierarchical modeling contexts such as volatility dynamics. To estimate the parameters via maximum likelihood, we numerically invert the characteristic function, as the probability density function lacks a closed-form expression. Parameters are then estimated by maximizing the log-likelihood using numerical optimization techniques (BFGS).

4.2.9. Comparison between power-law distributions and the generalized beta of the second kind (GB2) family. One might argue that the comparison of power-law distributions with the exponential and log-normal distributions introduced in Section 4.1.1 does not provide an informative benchmark for evaluating the appropriateness of the power-law model. As a consequence, we consider the Generalized Beta of the Second Kind (GB2) family as a more flexible alternative, as it accommodates both fat tails and finite second moments across a wide range of parameterizations. The GB2 is a highly flexible, four-parameter family of continuous probability distributions that can represent a wide variety of shapes, including both heavy-tailed and light-tailed forms. It is frequently employed in the analysis of skewed or heavy-tailed data. The GB2 distribution is defined as:

$$f(x; a; b; p; q) = \frac{a(x/b)^{ap-1}}{bB(p,q)[1 + (x/b)^a]^{p+q}}, \tag{26}$$

where $B(p, q)$ denotes the Beta function, $a > 0$ is the tail parameter controlling the tail heaviness, $b > 0$ is a scale parameter, and $p > 0$, $q > 0$ determine the shape of the distribution, including skewness. In Table A.5 of the appendix, we list several important subfamilies of the GB2 distribution, highlighting its role as a 'distributional umbrella' that encompasses many well-known distributions. Asymptotically, the GB2 exhibits power-law decay under certain conditions:

$$P(X > x) \sim x^{-aq}, \tag{27}$$

as $x \to \infty$, indicating that the product aq serves as an effective tail exponent, thereby linking the GB2 to power-law modeling. For a valid comparison between the GB2 and power-law models, both must be estimated using maximum likelihood, and the likelihoods must be evaluated over the same data range—specifically, the range above the power-law cutoff x_{MIN}. Accordingly, we restrict the GB2 model to the same data ranges used for the power-law estimation, as reported in table 3. We then compute the log-likelihood values and the corresponding AIC for each model.

5. Results

5.1. Main results

This section presents the findings from our analysis, applying the methodological approach outlined in Section 4.1 to the selected financial assets: S&P 500, gold, crude oil, USD/GBP exchange rate, and Bitcoin.

The analysis begins by modeling the Garman-Klass range-based variances using the power-law function described in Section 4.1.1. Table 2 highlights the share of cumulative total variance contributed by the top 1% and top 20% of observations for each asset, revealing a significant concentration. A small proportion of extreme observations accounts for a disproportionate share of total variance, consistent with the heavy-tailed behavior expected under a power-law distribution. For instance, among the top 1% of observations, crude oil exhibits the highest concentration at 27.23%, followed by Bitcoin (20.03%), S&P 500 (16.10%), gold (15.05%), and USD/GBP exchange rate (14.39%). Similarly, for the top 20%, Bitcoin leads with 72.03%, followed by crude oil (66.15%), S&P 500 (65.91%), gold (63.00%), and USD/GBP exchange rate (55.45%). These results underscore the presence of extreme events driving range-based variances, particularly in crude oil and Bitcoin, aligning with the Pareto 80/20 rule.

Next, a power-law distribution is fitted to the annualized daily range-based variances of each asset using MLE, as detailed in Section 4.1.1 and proposed by White *et al.* (2008) and Clauset *et al.* (2009). Table 3 reports the tail exponents, ranging from $\hat{\alpha} = 2.62$ for crude oil to $\hat{\alpha} = 2.94$ for the S&P 500, indicating that variance of variance is infinite for all assets. Such heavy tails invalidate foundational assumptions underlying conventional statistical tools like *t*-tests, which depend on finite variances. Standard metrics derived from ordinary least squares regression, such as *t*-statistics, become unreliable due to their sample-specific dependency. The evidence confirms that heavy-tailed distributions render traditional econometric methods inadequate, consistent with critiques by Grobys (2021) and Fathi *et al.* (2025).

To further validate the plausibility of the power-law model, goodness-of-fit tests (Clauset *et al.* 2009) are applied to assess the plausibility of power-law and alternative distributions, including log-normal and exponential models. Table 4 reports *p*-values for these tests, demonstrating strong support for the power-law model, as all *p*-values for the null hypothesis of a power-law distribution exceed 5%. In contrast, the log-normal model is rejected outright ($p = 0.00$) for all assets except Bitcoin, where the power-law model ($p = 0.66$) outperforms log-normal ($p = 0.52$). The exponential model is conclusively ruled out, with *p*-values equating to zero for all cases. These results collectively confirm the superior fit of the power-law model to the data.

A joint test, described in Section 4.1.2, examines whether the Garman-Klass range-based variances exhibit a shared component characterized by a common power-law exponent. To account for dependencies such as volatility clustering, block bootstrap methods are employed, yielding robust standard errors. Table 5 illustrates the increased standard deviations derived from bootstrapping. For instance, the standard deviation for S&P 500 increases from 0.05 to 0.20, and for gold, from 0.06 to 0.14. These adjustments underscore the critical importance of incorporating dependency structures in estimating tail exponents.

Subsequently, the joint test evaluates whether the assets share a common power-law exponent. From table 6, the test statistic $\hat{\lambda}$, computed iteratively over a range of α-values

Table 2. Share of the top 1% and top 20%.

Metric	S&*P* 500	Gold	Crude oil	USD/GBP	BTC
Top 1% Share	16.10%	15.05%	27.23%	14.39%	20.03%
Top 20% Share	65.91%	63.00%	66.15%	55.45%	72.03%

Note: This table displays the share of the cumulative total represented by the top 1% and top 20% of the distribution for the annualized daily Garman-Klass range-based variance across the S&*P* 500, gold, crude oil, the USD/GBP exchange rate, and Bitcoin.

Table 3. Estimation of power-law exponents for annualized daily range-based variance.

Metric	S&*P* 500	Gold	Crude oil	USD/GBP	BTC
$\hat{\alpha}$	2.94	2.74	2.62	2.78	2.84
$\hat{x}_{MIN}$	4.59	6.62	23.97	1.09	187.71
D	0.02	0.02	0.02	0.01	0.04
N_{PL}	11.93%	8.33%	10.30%	22.77%	3.41%
Std. Dev	0.05	0.06	0.05	0.04	0.17
Observations	11207	11196	8556	6263	3603
Period (MM/DD/YYYY)	02/19/1980	02/07/1980	01/02/1991	07/25/2000	09/17/2014
	07/31/2024	07/31/2024	07/31/2024	07/31/2024	07/31/2024

Note: This table presents the estimation results for power-law exponents applied to the annualized daily range-based variances of the S&*P* 500, gold, crude oil, the USD/GBP exchange rate, and Bitcoin. The parameter $\hat{\alpha}$ signifies the estimated tail exponent, while $\hat{\sigma}$ denotes the estimated standard deviation. The lower threshold $\hat{x}_{MIN}$ is identified through the optimized Kolmogorov-Smirnov distance (D), following the procedure described by Clauset *et al.* (2009). The reported $\hat{x}_{MIN}$ corresponds to the optimal distance D. Additionally, the fraction of observations obtained by the power-law process, denoted as N_{PL} is provided for each asset.

Table 4. Goodness-of-fit tests for the annualized daily range-based variance.

Asset	Power-law	Log-normal	Exponential
S&*P* 500	0.25	0.00	0.00
Gold	0.39	0.00	0.00
Crude oil	0.40	0.00	0.00
USD/GBP	0.46	0.00	0.00
BTC	0.66	0.52	0.00

Note: This table presents the results of the goodness-of-fit tests conducted using the Kolmogorov-Smirnov (KS) method to assess whether the empirical data and synthetic data generated from a power-law distribution, specified by x_{min} and α, originate from the same underlying distribution (column 2). Additionally, the table includes the results of goodness-of-fit tests for log-normal and exponential distributions in columns 3 and 4, respectively. The null hypothesis for these tests states that the empirical data and the synthetic data generated from the specified distributions (log-normal and exponential) are consistent, suggesting that each distribution provides an acceptable fit to the observed data.

from 1.2 to 3.2, fails to reject the null hypothesis of a shared exponent within the economically important range of $2.5 < \alpha < 3.1$. This finding suggests a unified component influencing variances. Notably, our results suggest that $\hat{\alpha} \approx 2.8$ produces the highest p-value ($p = 0.87$), which indicates that the second moment of the common power law governing the variance risk of unrelated financial asset markets is, statistically, infinite.

5.2. Results from robustness checks

To ensure the observed power-law behavior is not an artifact of statistical effects such as autocorrelation, robustness checks are performed. As discussed in Section 4.2.1, autoregressive models of order p are fitted to each asset's Garman-Klass range-based variance. Table 7 reports the point estimates, confirming significant autocorrelation across all assets, with partial autocorrelation functions indicating orders of $p = 2$, 6, 1, 4 for S&P 500, gold, crude oil, USD/GBP exchange rate, and Bitcoin, respectively. Descriptive statistics for the resulting innovation processes, detailed in table 8, reveal extremely heavy tails. For instance, kurtosis values range from 133.83 for Bitcoin to 8053.8 for crude oil, reinforcing the persistence of extreme values even after autoregressive adjustments.

Table 9 presents power-law exponents derived from the absolute innovation processes, closely matching those in table 3, further substantiating the presence of genuine power-law behavior. The goodness-of-fit tests applied to the innovation processes (table 10) corroborate these findings, failing to reject the power-law null hypothesis for all assets except gold, where the evidence is slightly weaker. Log-normal and exponential distributions are once again rejected outright ($p = 0.00$) across all assets.

Next, sample-split tests are conducted to validate the robustness of power-law characteristics across subsamples. Table 11 provides power-law exponent estimates for non-overlapping subsamples, demonstrating consistent statistical

Table 5. Descriptive statistics for the power-law exponents estimated using block bootstrap methods.

Statistic	$\hat{\alpha}^{boot}_{\text{S\&P 500}}$	$\hat{\alpha}^{boot}_{Gold}$	$\hat{\alpha}^{boot}_{Crudeoil}$	$\hat{\alpha}^{boot}_{USD/GBP}$	$\hat{\alpha}^{boot}_{BTC}$
Mean	2.95	2.74	2.61	2.81	2.33
Median	2.95	2.74	2.59	2.79	2.27
Maximum	3.57	3.37	3.48	3.75	3.44
Minimum	2.38	2.37	2.26	2.38	1.91
Std. Dev	0.20	0.14	0.17	0.18	0.25
Skewness	0.01	0.31	1.01	0.88	1.63
Kurtosis	2.80	3.42	4.94	4.51	5.93
Jarque-Bera (JB)	1.70	23.08	326.81	225.13	802.29
(p-value) $_{\text{JB}}$	0.41	0.00	0.00	0.00	0.00
Observations	11207	11196	8557	6263	3603

Note: This table reports the block bootstrap methodology test to the annualized daily range-based variance for the S&*P* 500, gold, crude oil, USD/GBP exchange rate, and Bitcoin. The block bootstrap procedure is implemented with the block length m, where $E[m] = T^{1/3}$ following the recommendation by Godfrey (2009) for variance estimation. From the given data vector $\mathbf{x}$, blocks of size m are randomly selected, where m follows a geometric distribution $m \sim GEO(p)$ with an expected value $E[m] = \frac{(1-p)}{p}$. Thus, in the overall data sample, we use $p = 0.0435$, $p = 0.0434$, $p = 0.0476$, $p = 0.0526$ and $p = 0.0625$ for the range-based variances of the S&*P* 500, gold, crude oil, USD/GBP exchange rate, and Bitcoin, respectively. Using this bootstrap method, blocks drawn from the data vector x have varying lengths. The randomly selected blocks, m, are then stacked into a new vector

$$\boldsymbol{x}_i^b = \begin{bmatrix} m_1 \\ m_2 \\ m_3 \\ \vdots \end{bmatrix}$$

where the lengths of the blocks $m_1, m_2, \ldots$ vary. The process continues until the length of the constructed vector $\mathbf{x}^b$ exceeds T. Then, we cut off any observations exceeding T, ensuring that the artificial data vector $\boldsymbol{x}^b$ matches the length of the original data vector $\boldsymbol{x}$. By applying this blocks bootstrap, 1000 artificial data vectors $\begin{bmatrix} \boldsymbol{x}^1 & \boldsymbol{x}^2 & \cdots & \boldsymbol{x}^B \end{bmatrix}$, are generated for each given original data vector. Next, the point estimates $\hat{\alpha}$ for each bootstrap data vector $\begin{bmatrix} \boldsymbol{x}^1 & \boldsymbol{x}^2 & \cdots & \boldsymbol{x}^B \end{bmatrix}$, are calculated and stored in a vector $\begin{bmatrix} \hat{\alpha}^1 & \hat{\alpha}^2 & \cdots & \hat{\alpha}^B \end{bmatrix}$ following the method described by Clauset *et al.* (2009). The block bootstrap method is described in detail in Section 3.1.2.

Table 6. Testing for a common power-law exponent governing from annualized daily range-based variance.

q	$\hat{\lambda}$	p-value
1.2	390.68	**0.00**
1.3	342.52	**0.00**
1.4	297.53	**0.00**
1.5	255.73	**0.00**
1.6	217.11	**0.00**
1.7	181.68	**0.00**
1.8	149.42	**0.00**
1.9	120.34	**0.00**
2	94.45	**0.00**
2.1	71.74	**0.00**
2.2	52.21	**0.00**
2.3	35.87	**0.00**
2.4	22.70	**0.00**
2.5	12.72	**0.03**
2.6	5.91	0.31
2.7	2.29	0.81
2.8	1.85	0.87
2.9	4.60	0.47
3	10.52	0.06
3.1	19.63	**0.00**
3.2	31.92	**0.00**

Note: This table presents the results of a joint test designed to assess whether the range-based variances of S&*P* 500, gold, crude oil, USD/GBP exchange rate, and Bitcoin share a common component. To investigate whether a common component underlies the power-law behavior of these assets, the following test statistic is utilized:

$$\hat{\lambda} = (\hat{\boldsymbol{\alpha}} - q\mathbf{1})' \hat{\boldsymbol{\Sigma}}_{\hat{\boldsymbol{\alpha}}}^{-1} (\hat{\boldsymbol{\alpha}} - q\mathbf{1}),$$

where $\hat{\boldsymbol{\Sigma}}_{\hat{\boldsymbol{\alpha}}}$ is the estimated 5×5 covariance matrix, $\hat{\boldsymbol{\alpha}}$ is a 5×1 vector of estimated power-law exponents, $\mathbf{1}$ is a 5×1 vector of ones, and q represents the hypothesized power-law exponent. The test statistic $\hat{\lambda}$ follows a $\chi^2(5)$ distribution under the null hypothesis. The statistic is iteratively calculated across the economically significant range of $q = (1.2,\ 1.3, \ldots,\ 3.1,\ 3.2)$. Bolded values in the results represents statistical significance at the 5% level.

properties across both panels. Exceptions include the S&P 500 in Panel A and gold in Panel B, where the goodness-of-fit test rejects the power-law hypothesis. Nevertheless, the log-normal and exponential models remain consistently rejected across all subsamples ($p = 0.00$). This consistency across tests and subsamples strengthens the conclusion that genuine power-law behavior governs the range-based variances of these financial assets.

Building on the robustness analysis outlined in Section 4.2.3, we report the results derived from the weekly realized variance estimator in this section. Table A.1 presents the descriptive statistics for the weekly realized variances across the five asset classes. Consistent with our earlier findings, the realized variance distributions exhibit substantial skewness and excess kurtosis—hallmarks of heavy-tailed behavior. Weekly realized variances for crude oil and Bitcoin, in particular, display considerable variation and extreme upper-tail values, further supporting the presence of volatility clustering and rare but impactful events. We then estimate power-law exponents for the tail behavior of the weekly realized variances using the MLE approach proposed by Clauset *et al*. (2009). As reported in Table A.2 the estimated exponents all lie within the critical range $2 < \hat{\alpha} < 3$, confirming that the variance of variance remains theoretically undefined for all asset markets. These results align closely with those obtained using the Garman-Klass estimator, indicating that our primary conclusions are not sensitive to the choice of volatility measure. To further validate the plausibility of the power-law model under this alternative volatility measure, we conduct KS goodness-of-fit tests for power-law, log-normal, and exponential distributions (Table A.3). Based on the results in Table A.3, the power-law model remains statistically plausible for all assets (p-values > 0.05), except gold, while the exponential model is decisively rejected across all the assets. Additionally, although the log-normal model is also accepted for all assets (p-values > 0.05), the power-law model generally provides a superior fit, as reflected in higher p-values—except in the case of gold. In summary, the persistence of power-law behavior under both range-based and return-based volatility estimators confirms the robustness of our core results. These findings also underscore the broader insight that volatility risk in financial markets may be governed by a common, heavy-tailed structure—regardless of the specific estimation method employed.

Additionally, as described in Section 4.2.4, we extended the analysis to incorporate government bond markets in order to examine whether the statistical properties of realized variances also apply to U.S. Treasury yields with 2-year, 5-year, and 10-year maturities. This extension allows us to assess the broader applicability of power-law behavior to fixed income markets. The results of this extended analysis are presented in tables 12–14. As shown in table 12, the descriptive statistics for the range-based variances of the 2-year, 5-year, and

Table 7. Point estimates for autoregressive models of for annualized daily range-based variance.

	$\hat{\beta}_{0,j}$	$\hat{\beta}_{1,j}$	$\hat{\beta}_{2,j}$	$\hat{\beta}_{3,j}$	$\hat{\beta}_{4,j}$	$\hat{\beta}_{5,j}$	$\hat{\beta}_{6,j}$	R^2
$\hat{\sigma}^2_{S\&P500,t}$	0.49***	0.42***	0.10	0.08***	0.18***			0.42
	(12.27)	(44.89)	(10.33)	(7.81)	(18.90)			
$\hat{\sigma}^2_{Gold,t}$	0.74***	0.36***	0.07**	0.03*	0.11***	0.08***	0.09***	0.30
	(7.33)	(8.71)	(2.53)	(1.69)	(2.64)	(2.95)	(3.58)	
$\hat{\sigma}^2_{Crudeoil,t}$	13.34***	0.08***						0.01
	(6.09)	(3.37)						
$\hat{\sigma}^2_{USD/GBP,t}$	0.48***	0.16***	0.13**	0.09***	0.11***			0.10
	(3.52)	(3.11)	(2.11)	(3.29)	(3.12)			
$\hat{\sigma}^2_{BTC,t}$	20.35***	0.44***						0.19
	(10.73)	(9.93)						

*, ** and *** indicate statistical significance at the 10%, 5% and 1% levels, respectively.
Note: This table presents the estimated coefficients from autoregressive models of order P fitted to the annualized daily range-based variance for the S&P 500, gold, crude oil, the USD/GBP exchange rate, and Bitcoin (BTC). The models are specified as

$$\hat{\sigma}^2_{j,t} = \beta_{0,j} + \beta_{1,j}\hat{\sigma}^2_{j,t-1} + \beta_{2,j}\hat{\sigma}^2_{j,t-2} + \ldots + \beta_{p,j}\hat{\sigma}^2_{j,t-p} + \varepsilon_{j,t},$$

where $\varepsilon_{j,t}$ is the innovation process, j refers to the respective asset. The optimal lag order P is determined by the partial autocorrelation function. The reported coefficients include the intercept $\hat{\beta}_{0,j}$ and autoregressive terms ($\beta_{0,j}, \beta_{1,j}, \beta_{2,j}, \ldots, \beta_{p,j}$). The t-statistics are reported in parentheses.

Table 8. Descriptive statistics for the innovations process of annualized daily range-based variance.

Statistic	$\hat{\boldsymbol{\varepsilon}}_{S\&P500}$	$\hat{\boldsymbol{\varepsilon}}_{Gold}$	$\hat{\boldsymbol{\varepsilon}}_{Crudeoil}$	$\hat{\boldsymbol{\varepsilon}}_{USD/GBP}$	$\hat{\boldsymbol{\varepsilon}}_{BTC}$
Mean	0.00	0.00	0.00	0.00	0.00
Median	− 0.40	− 0.63	− 7.14	− 0.24	− 14.29
Maximum	139.02	163.67	15818.40	132.17	1750.00
Minimum	− 70.72	− 56.60	− 1048.3	− 21.49	− 676.04
Std. Dev	3.68	4.64	173.62	2.20	80.99
Skewness	11.83	10.18	88.46	38.32	8.33
Kurtosis	377.28	250.67	8053.8	2145.90	133.83
Observations	11203	11190	8555	6259	3602

Note: This table summarizes the descriptive statistics for the innovation process $\varepsilon_{i,t}$ of the annualized daily range-based variance for the S&P 500, gold, crude oil, the USD/GBP exchange rate, and Bitcoin (BTC), as reported in Table 3. The innovation process of annualized daily range-based variances for all five key assets is estimated by running autoregressive models of order p:

$$\hat{\sigma}^2_{j,t} = \beta_{0,j} + \beta_{1,j}\hat{\sigma}^2_{j,t-1} + \beta_{2,j}\hat{\sigma}^2_{j,t-2} + \ldots + \beta_{p,j}\hat{\sigma}^2_{j,t-p} + \varepsilon_{j,t},$$

where $\varepsilon_{j,t}$ is the innovation process, p is the lag-order, j refers to the respective asset. The optimal lag order p is determined through an analysis of the partial autocorrelation function.

10-year Treasury yields exhibit high levels of skewness and kurtosis, indicating heavy-tailed distributions similar to those observed in the five major financial asset markets. The power-law estimation results (table 13) show tail exponents of U.S. Treasury yields with 2-year, 5-year, and 10-year maturities, all falling within the critical interval $2 < \hat{\alpha} < 3$. This implies that the second moment of range-based variances for these bonds remains undefined, in line with our findings for major financial asset markets. In addition, goodness-of-fit test results in table 14 further confirm the plausibility of the power-law model for bond market variances. The null hypothesis of a power-law distribution is not rejected for any of the three bond series (p-values: 0.94, 0.54, and 0.58, respectively). In contrast, the log-normal and exponential models are decisively rejected for all three bond series. These results provide compelling evidence that power-law behavior is a persistent and robust characteristic of range-based variances across diverse financial markets—including government bond markets. This suggests that heavy-tailed variance risk may be a universal feature of modern financial systems, further reinforcing the need to reconsider traditional models based on finite-variance assumptions.

Next, to complement our primary estimation strategy and assess the robustness of the results, we apply a Bayesian inference approach to estimate the power-law parameters across all assets as described in section 4.2.5. Table 15 reports the Bayesian estimates of the power-law exponent $\hat{\alpha}$, the inferred lower-bound $\hat{x}_{min}$. The results confirm that all

Table 9. Estimating power-law exponents for the absolute amount of the innovation processes of the annualized daily range-based variance.

Metric	$\lvert\hat{\varepsilon}_{S\&P500}\rvert$	$\lvert\hat{\varepsilon}_{Gold}\rvert$	$\lvert\hat{\varepsilon}_{Crudeoil}\rvert$	$\lvert\hat{\varepsilon}_{USD/GBP}\rvert$	$\lvert\hat{\varepsilon}_{BTC}\rvert$
$\hat{\alpha}$	2.54	2.46	2.41	2.40	2.30
$\hat{x}_{MIN}$	3.71	2.81	40.90	1.12	56.55
D	0.02	0.02	0.03	0.03	0.04
N_{PL}	5.51%	14.59%	2.58%	6.65%	9.69%
Std. Dev	0.06	0.04	0.09	0.07	0.07
Observations	11203	11190	8555	6259	3602

Note: This table presents the estimation results for the power-law exponents applied to the absolute amount of the residual series of annualized daily range-based variances for the S&*P* 500, gold, crude oil, the exchange rate of the U.S. dollar and Bitcoin (BTC). The innovation process for each asset is obtained by using the following autoregressive model:

$$\hat{\sigma}^2_{j,t} = \beta_{0,j} + \beta_{1,j}\hat{\sigma}^2_{j,t-1} + \beta_{2,j}\hat{\sigma}^2_{j,t-2} + \ldots + \beta_{p,j}\hat{\sigma}^2_{j,t-p} + \varepsilon_{j,t}$$

where $\varepsilon_{j,t}$ is the innovation process, p is the lag-order, and j refers to the respective asset. The parameter $\hat{\alpha}$ represents the estimated tail exponent, while $\hat{\sigma}$ denotes the estimated standard deviation. The lower threshold $\hat{x}_{MIN}$ is determined using the optimized Kolmogorov-Smirnov distance (D) approach, as outlined by Clauset *et al*. (2009). The reported $\hat{x}_{MIN}$ corresponds to the optimal distance D. Additionally, the fraction of observations governed by the power-law process, denoted as N_{PL} is provided for each asset.

Table 10. Goodness-of-fit tests for the innovation processes of annualized daily range-based variance.

	Power-law	Log-normal	Exponential
$\lvert\hat{\varepsilon}_{S\&P500}\rvert$	0.82	0.00	0.00
$\lvert\hat{\varepsilon}_{Gold}\rvert$	0.02	0.00	0.00
$\lvert\hat{\varepsilon}_{Crudeoil}\rvert$	0.88	0.00	0.00
$\lvert\hat{\varepsilon}_{USD/GBP}\rvert$	0.22	0.00	0.00
$\lvert\hat{\varepsilon}_{BTC}\rvert$	0.07	0.00	0.00

Note: This table presents the results of the goodness-of-fit tests conducted using the Kolmogorov-Smirnov (KS) method to assess whether the empirical data and synthetic data generated from a power-law distribution, specified by x_{min} and α, originate from the same underlying distribution (column 2). Additionally, the table includes the results of goodness-of-fit tests for log-normal and exponential distributions in columns 3 and 4, respectively. The null hypothesis for these tests states that the empirical data and the synthetic data generated from the specified distributions (log-normal and exponential) are consistent, suggesting that each distribution provides an acceptable fit to the observed data.

estimated exponents fall within the range typically associated with heavy-tailed behavior $2 < \hat{\alpha} < 3$, consistent with our main findings based on Clauset *et al*.'s (2009) approach. Importantly, the 95% credible intervals for $\hat{\alpha}$ across all assets are relatively narrow, indicating precise and stable estimates of the power-law exponent under the Bayesian framework. In addition, figure 1 visualizes the posterior distribution of the power-law exponent $\hat{\alpha}$ for each asset, illustrating the concentration of posterior mass around the mean and the precision of the Bayesian estimates. This robustness reinforces the credibility of our earlier conclusions regarding tail behavior in financial range-based variances.

To complement the goodness-of-fit tests, we conducted a formal model comparison using the AIC, as described in Section 4.2.6. The AIC accounts for both model fit and complexity, with lower values indicating a more parsimonious and better-fitting model. Each distribution—power-law, log-normal, and exponential—was fitted to the empirical data using MLE. Table 16 reports the AIC values for each model across the five asset classes. In all cases, the power-law distribution produces the lowest AIC, indicating a superior fit to the extreme tails of the range-based variance distributions when compared to the log-normal and exponential alternatives. These findings provide consistent and robust evidence that power-law models are better suited to capture the heavy-tailed nature of range-based asset variance distributions. The results reinforce the conclusions drawn from the goodness-of-fit tests and underscore the relevance of power-law behavior in modeling extreme financial events.

Furthermore, the results of the rolling-window estimations outlined in Section 4.2.7 are presented in Table A.4 while Figure A.1 visualizes the evolution of the time-varying power-law exponents over the sample period. Notably, the S&P 500 dataset contains $T = 11\,207$ observations of range-based variance, allowing for the estimation of $N = 205$ power-law exponents. In contrast, for Bitcoin, only $N = 53$ exponents could be estimated due to the shorter sample. A comparison between the full-sample estimates (table 3) and the rolling window medians (Table A.4) reveals close alignment. For example, Table A.4 reports median power-law exponents of 2.73 and 2.77 for the S&P 500 and Gold, respectively, while the corresponding full-sample point estimates in table 3 are 2.94 and 2.74. Similar consistency is observed across other range-based variance series. Finally, a visual inspection of Figure A.1 suggests that the time-varying power-law exponents derived from the rolling window estimation appear stationary, reinforcing the conclusion that the exponent estimates are stable—that is, converging.

Next, we fit tempered stable distributions, as outlined in Section 4.2.8, to the range-based variances of the S&P 500, USD/GBP exchange rate, gold, crude oil, and Bitcoin, initially fixing the power-law exponent $\alpha_i = \alpha = 2.8$. The results

Table 11. Sample split analysis of power-law exponents for the innovation processes of annualized daily range-based variance.

Panel A: Estimation results for the first subsample of power-law exponents and related metrics.					
Metric	S&P 500	Gold	Crude oil	USD/GBP	BTC
$\hat{\alpha}$	2.18	2.48	2.29	2.30	2.44
$\hat{x}_{MIN}$	0.65	2.82	33.07	1.24	26.81
$(p\text{-value})_{\text{power-law}}$	0.00	0.27	0.28	0.96	0.10
D	0.02	0.02	0.04	0.03	0.04
N_{PL}	48.79	16.93	5.10	5.08	18.17
Std. Dev	0.02	0.05	0.09	0.10	0.08
$(p\text{-value})_{\text{log-normal}}$	0.00	0.00	0.00	0.00	0.00
$(p\text{-value})_{\text{exponential}}$	0.00	0.00	0.00	0.00	0.00
Observations	5601	5595	4277	3129	1801
Panel B: Estimation results for the second subsample of power-law exponents and related metrics.					
Metric	S&P 500	Gold	Crude oil	USD/GBP	BTC
$\hat{\alpha}$	2.76	2.31	2.49	2.47	2.21
$\hat{x}_{MIN}$	3.13	1.04	13.42	0.92	49.73
$(p\text{-value})_{\text{power-law}}$	0.85	0.00	0.39	0.12	0.40
D	0.02	0.02	0.04	0.04	0.03
N_{PL}	7.10	43.66	5.35	9.90	14.71
Std. Dev	0.09	0.03	0.10	0.08	0.07
$(p\text{-value})_{\text{log-normal}}$	0.00	0.00	0.00	0.00	0.00
$(p\text{-value})_{\text{exponential}}$	0.00	0.00	0.00	0.00	0.00
Observations	5602	5595	4278	3130	1801

Note: This table presents the sample-split test of power-law exponents applied to the residual series of annualized daily range-based variances, with results divided into two subsamples: Panel A reports the first subsample, and Panel B reports the second subsample. The parameter $\hat{\alpha}$ represents the estimated tail exponent, while $\hat{\sigma}$ denotes the estimated standard deviation. The lower threshold $\hat{x}_{MIN}$ is determined using the optimized Kolmogorov-Smirnov distance (D) approach, as outlined by Clauset *et al*. (2009). The reported $\hat{x}_{MIN}$ corresponds to the optimal distance D. Additionally, the fraction of observations obtained by the power-law process, denoted as N_{PL} is provided for each asset.

Table 12. Descriptive statistics of range-based U.S. Treasury yield variances.

Statistic	UST 2Y	UST 5Y	UST 10Y
Mean	51.41	35.47	21.70
Median	14.50	12.28	6.97
Maximum	3042.13	2975.99	5041.98
Minimum	0.00	0.00	0.00
Std. Dev.	157.46	114.40	120.87
Skewness	10.02	12.83	28.73
Kurtosis	133.63	233.29	1087.59
Observations	3010	3033	2818
Period (MM/DD/YYYY)	10/26/2012	10/26/2012	08/26/2013
	07/31/2024	07/31/2024	07/31/2024

Note: This table presents the descriptive statistics of the annualized daily range-based variances for U.S. Treasury yields with maturities of 2 years (UST 2Y), 5 years (UST 5Y), and 10 years (UST 10Y). The variances are calculated using the Garman-Klass estimator, based on daily high, low, open, and close yields.

reveal that λ_i could be estimated only for the range-based variance for the USD/GBP exchange rate, while the estimation failed to converge for the remaining series. To validate this finding, we repeated the estimation without constraining α. Again, both α_i and λ_i could be reliably estimated only for the range-based variance for the USD/GBP series. This pattern is highly informative. It suggests that, for most assets, the data do not exhibit statistically significant exponential truncation in the tails. Rather, the data appear to conform closely to a pure power law over the observed range, rendering the inclusion of a tempering parameter either superfluous or numerically unstable. This interpretation aligns with earlier empirical evidence of strong power-law decay in these series. The consistent failure to estimate λ_i even when α_i is unconstrained further supports the conclusion that the tail behavior is well captured by a standard power law without the need for exponential tempering.

Finally, restricting the data to $x \geq x_{MIN}$, we fit GB2 models to the range-based variances and computed the AIC values, as outlined in Section 4.2.9. Table 17 presents the

Table 13. Estimation of power-law exponents for range-based U.S. Treasury yield variances.

Metric	UST 2Y	UST 5Y	UST 10Y
$\hat{\alpha}$	2.30	2.31	2.32
$\hat{x}_{MIN}$	87.42	56.62	27.45
D	0.02	0.03	0.02
N_{PL}	12.82%	12.43%	14.05%
Std. Dev	0.07	0.07	0.07
Observations	3010	3033	2818
Period (MM/DD/YYYY)	02/19/1980	02/07/1980	01/02/1991
	07/31/2024	07/31/2024	07/31/2024

Note: This table presents the estimation results for power-law exponents applied to the annualized daily range-based variances of U.S. Treasury yields with 2-year (UST 2Y), 5-year (UST 5Y), and 10-year (UST 10Y) maturities. The parameter $\hat{\alpha}$ signifies the estimated tail exponent, while $\hat{\sigma}$ denotes the estimated standard deviation. The lower threshold $\hat{x}_{MIN}$ is identified through the optimized Kolmogorov-Smirnov distance (D), following the procedure described by Clauset *et al.* (2009). The reported $\hat{x}_{MIN}$ corresponds to the optimal distance D. Additionally, the fraction of observations obtained by the power-law process, denoted as N_{PL} is provided for each bond.

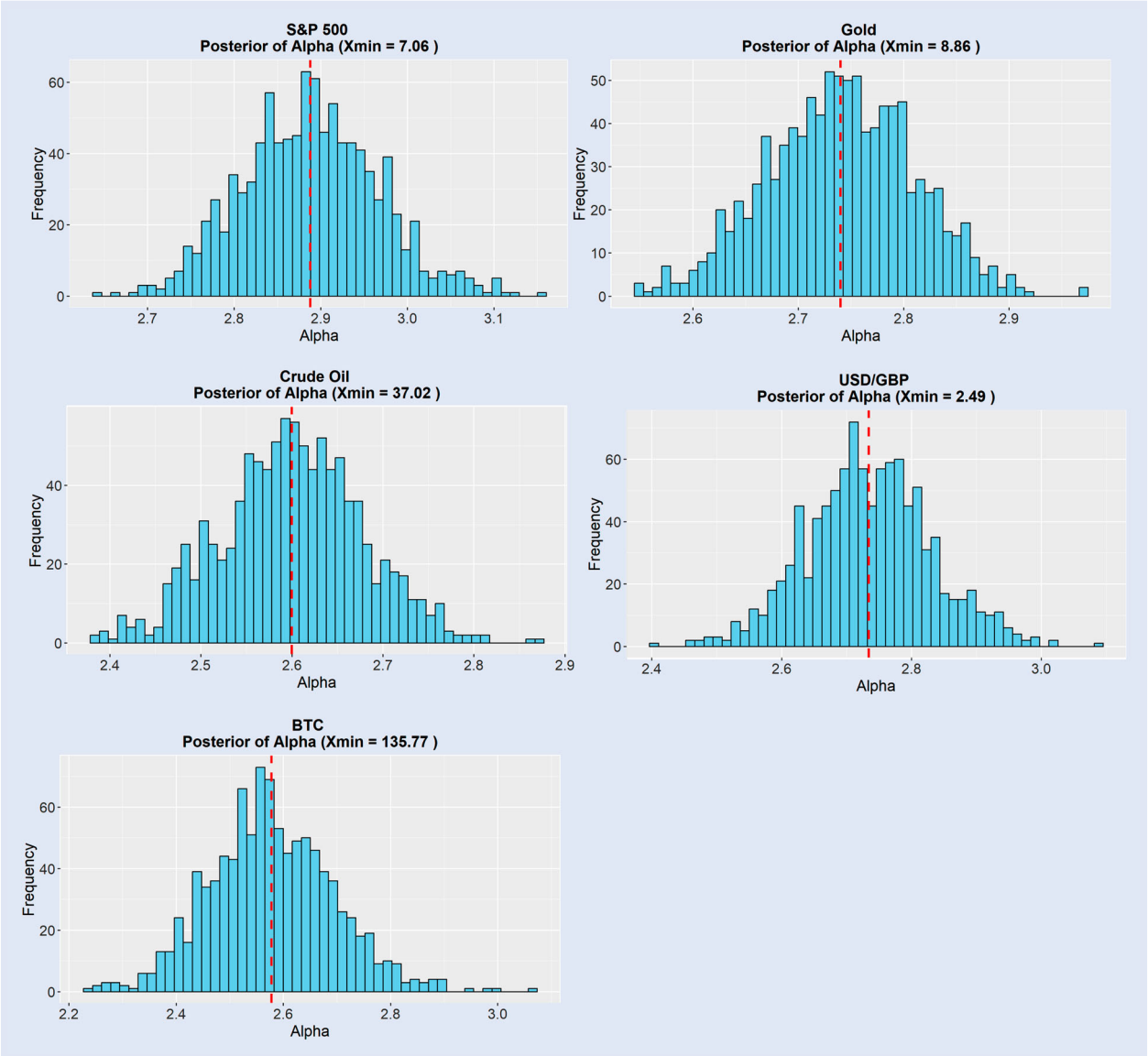

Figure 1. Posterior distribution of the power-law exponent $\hat{\alpha}$, estimated using Bayesian inference. Note: This figure shows the posterior distribution of the power-law exponent $\hat{\alpha}$, estimated using Bayesian inference for values greater than the threshold $\hat{x}_{min}$. The red dashed line indicates the posterior mean of $\hat{\alpha}$.

Table 14. Goodness-of-fit tests for range-based U.S. Treasury yield variances.

Asset	Power-law	Log-normal	Exponential
UST 2Y	0.94	0.04	0.00
UST 5Y	0.54	0.00	0.00
UST 10Y	0.58	0.00	0.00

Note: This table reports the results (viz., p-values) of the goodness-of-fit tests for the annualized daily range-based variances of U.S. Treasury yields with maturities of 2 years (UST 2Y), 5 years (UST 5Y), and 10 years (UST 10Y). The tests are conducted using the Kolmogorov-Smirnov (KS) method to assess whether the empirical data and the synthetic data—generated from a power-law distribution specified by x_{min} and α —originate from the same underlying distribution (column 2). Additionally, the table includes the results of goodness-of-fit tests for log-normal and exponential distributions in columns 3 and 4, respectively. The null hypothesis for these tests states that the empirical data and the synthetic data generated from the specified distributions (log-normal and exponential) are consistent, suggesting that each distribution provides an acceptable fit to the observed data.

log-likelihoods and AIC values for both the power-law models—using the parameterizations from table 3—and the GB2 models restricted to the equivalent data ranges. Parameter estimates for the GB2 models are provided in Table A.6 in the appendix. The results in table 17 indicate that the AIC values are consistently lower for the power-law models across all range-based variance series, regardless of the underlying asset class. This finding reinforces the results of our main analysis, further supporting the conclusion that power-law models are particularly well suited for capturing the dynamics of range-based variances in financial assets.

6. Discussion

In this study we explored whether the Garman-Klass range-based variances of five key financial assets—S&P 500, gold, crude oil, USD/GBP exchange rate, and Bitcoin—follow power-law distributions and examined the broader implications of these findings for financial modeling and risk analysis. By utilizing the Garman-Klass variance estimator and conducting robust statistical tests, we provided a comprehensive analysis of power-law behavior in range-based variances of otherwise unrelated asset markets. Unlike previous studies that primarily focused on absolute returns or single-asset analyses, as highlighted by Lux and Alfarano (2016), we employ the Garman-Klass range-based variances, which provide greater sensitivity to intraday price dynamics and mitigate estimation bias. This methodological improvement enables us to capture the complexity of volatility structures across different asset classes more effectively.

First, we confirmed the heavy-tailed nature of range-based variances across all five assets, consistent with power-law behavior. Data on range-based asset variances exhibited

Table 15. Bayesian estimation for power-law exponents.

Metric	S&P 500	Gold	Crude oil	USD/GBP	BTC
$\hat{\alpha}$	2.89	2.74	2.60	2.73	2.58
$\hat{x}_{MIN}$	7.06	8.86	37.02	2.49	135.77
Std. Dev	0.08	0.07	0.08	0.09	0.12
CI $(\hat{\alpha})_{95\%}$	(2.73, 3.05)	(2.60, 2.88)	(2.44, 2.76)	(2.55, 2.91)	(2.34, 2.82)
Observations	11207	11196	8556	6263	3603
Period (MM/DD/YYYY)	02/19/1980	02/07/1980	01/02/1991	07/25/2000	09/17/2014
	07/31/2024	07/31/2024	07/31/2024	07/31/2024	07/31/2024

Note: This table presents the estimation results for power-law exponents using Bayesian approach applied to the annualized daily range-based variances of the S&P 500, gold, crude oil, the USD/GBP exchange rate, and Bitcoin (BTC). The table includes the posterior means of the exponent $\hat{\alpha}$ the estimated lower-bound threshold $\hat{x}_{min}$,the standard deviations of the posterior distributions for $\hat{\alpha}$, and the 95% credible intervals for $\hat{\alpha}$. The number of observations and the corresponding sample period for each asset are also provided.

Table 16. AIC model comparison.

Asset	Power-law*	Log-normal	Exponential
S&*P* 500	**6346.79**	36394.16	39929.06
Gold	**5433.58**	42811.29	45326.74
Crude oil	**7592.74**	58142.31	62010.57
USD/GBP	**3044.78**	10295.22	11925.14
BTC	**1518.62**	31259.29	33017.41

*Bold values indicate the best-fitting model by AIC.
Note: This table presents the AIC values for power-law, log-normal, and exponential distributions fitted to the annualized range-based variances for each five assets, including the S&*P* 500, gold, crude oil, USD/GBP exchange rate, and Bitcoin (BTC). Each model is estimated using maximum likelihood estimation methods. The AIC is calculated as $AIC = 2k - 2log(\hat{L})$, where k is the number of estimated parameters and $log(\hat{L})$ is the maximum log-likelihood of the model. Lower AIC values indicate a better trade-off between model fit and complexity.

Table 17. Comparison between power-law and GB2 functions.

Range-based variance	Log-likelihood Power law (AIC)	Log-likelihood GB2 (AIC)
S&*P* 500	–1134.28 (2268.57)	–3176.18 (6360.37)
Gold	–953.78 (1907.56)	–2714.71 (5437.42)
Crude oil	–996.82 (1993.63)	–3805.39 (7618.79)
USD/GBP	–1397.88 (2795.76)	–1528.31 (3064.61)
Bitcoin	–114.42 (228.85)	–782.70 (1573.40)

Note: We compare the GB2 distribution with our power-law models by fitting the GB2 function to the data range $x \geq x_{min}$ for each respective data vector, as reported in Table 3. The values of the log-likelihood functions are computed, along with the corresponding AIC. This table reports the log-likelihood and AIC values for both the power-law models—using the parameterizations documented in Table 3—and the GB2 models, which are estimated over the same data ranges defined by the respective power-law cutoffs.

significant skewness and kurtosis, with extreme values concentrated in the upper tails of the variance distributions. For example, Bitcoin exhibited the highest mean value of Garman-Klass range-based variance, reflecting its speculative and volatile nature, while the USD/GBP exchange rate displayed relatively lower mean value of Garman-Klass range-based variance.

Second, power-law fitting through MLE verified that tail exponents for all assets fell within the range $2 < \alpha < 3$, implying that the variance-of-variance is infinite. Interestingly, these findings contrast with literature from the early 1990s, as discussed by Lux and Alfarano (2016), which focused on the tail behavior of distributions and suggested that financial asset returns exhibit power-law behavior with finite variances. This result has profound implications, as it challenges traditional econometric assumptions that rely on finite variances for hypothesis testing. The estimated power-law exponent α has direct implications for economic risk. Lower values of α indicate heavier tails in the return distribution, implying a higher probability of extreme losses. This suggests a more volatile and risk-prone market environment. For instance, when α lies between 2 and 3, the theoretical mean of the variance process is defined but higher-order moments such as variance or skewness are undefined, posing challenges for traditional risk models. When α approaches 2 or below, the theoretical mean of the variance process becomes infinite, highlighting severe tail risk. Hence, the power-law exponent serves as a quantifiable indicator of the intensity of tail events, informing asset pricing, risk management, and regulatory capital frameworks.

This finding also aligns with the previous literature (Grobys 2021, 2023, 2024, Fathi *et al*. 2024, 2025) which documented tail exponents for realized variances or range-based variances are within the range $2 < \alpha < 3$, indicating that the variance-of-variances is infinite. In the presence of infinite variance-of-variance, extreme observations can disproportionately influence the variance estimate, leading to results that may appear significant in one sample but fail to replicate in others. As highlighted by Fama (1963), if variances are undefined, results derived from traditional statistical methods based on the concept of correlation (i.e. *t*-statistics) become inherently sample-dependent. According to Grobys (2021), unstable second moments lead to *t*-statistics that are highly dependent on the specific sample used. Thus, this study, in line with Grobys (2021), argues that the replication failures observed in financial research may stem from the infinite variance of variances, which leads to traditional statistical methods becoming unreliable.

Third, our results derived from goodness-of-fit tests strongly supported power-law distributions as plausible models for the range-based variances of these assets. These findings align with Mandelbrot's (1963) early insights that financial asset returns may lack finite variances, and strengthens the notion that traditional statistical tools, such as OLS and other moment-dependent methods, may be inadequate for modeling financial data governed by power-law distributions.

Fourth, our analysis comprehensively compared power-law distributions with alternative models (viz., log-normal and exponential). The goodness-of-fit test strongly supported power-law models as the most plausible representation of the data for all assets, with alternative distributions being consistently rejected. This finding strengthens the case for power-law distributions as a fundamental characteristic of financial asset variances. The rejection of log-normal and exponential models aligns with Taleb's (2020) view on the necessity of adopting power-law frameworks for analyzing financial data, particularly in the context of extreme events and tail risks. Furthermore, these findings contrast with the literature suggesting that realized asset volatility follows a log-normal distribution (e.g. Andersen *et al*. 2001, 2001a, 2001b), but they align with studies proposing that a Pareto distribution better describes volatility in financial markets (Renò and Rizza 2003, Grobys 2021, 2023, 2024, Fathi *et al*. 2024, 2025).

The presence of power-law behavior in financial returns and volatility carries profound implications for risk measurement frameworks such as Value-at-Risk (VaR) and stress testing. Traditional models, including those based on log-normal

or Gaussian assumptions, underestimate the probability and magnitude of extreme events due to their thin-tailed nature. Empirical evidence from Bouchaud (2001) and Gencay *et al.* (2003) demonstrates that financial markets often exhibit heavy-tailed distributions, particularly in the tails of return and variance distributions. This tail heaviness implies that large losses occur far more frequently than predicted by normal models, which can severely compromise the reliability of VaR estimates. Gencay and Selçuk (2004) show that applying Extreme Value Theory (EVT) and the Generalized Pareto Distribution (GPD) provides a more robust framework for modeling the tails of financial distributions. These approaches allow for better estimation of risk at high quantiles and facilitate more realistic stress testing scenarios. Moreover, power-law scaling properties are indicative of long memory and clustered volatility, which further challenge the assumptions of independence and stationarity in standard risk models. As such, incorporating power-law features into risk modeling frameworks is essential for accurately capturing the true nature of financial market risk, particularly in the context of systemic shocks.

Fifth, to assess whether the range-based variances of the five assets share a common component, we implemented a joint test hypothesizing a common power-law exponent. Recognizing the limitations of standard errors derived under independence assumptions of Clauset *et al.* (2009), we employed block bootstrap techniques following Grobys (2024) to compute robust standard errors. In line with the study of Grobys (2024), the bootstrap procedure showed that robust standard errors were significantly larger than the ones derived in the study of Clauset *et al.* (2009). Using the robust standard error, we carried out conjoint tests, iteratively computed across a range of hypothesized exponents (q). Our findings suggest strong evidence for a shared power-law exponent governing the range-based variances of these assets. Specifically, the null hypothesis of a shared exponent could not be rejected for the range $2.5 < q < 3.1$, suggesting a unified component influencing variance risks across the S&P 500, gold, crude oil, USD/GBP exchange rate, and Bitcoin. This finding aligns with theoretical expectations of power-law behavior and underscores the interconnected nature of these assets within a broader market framework.

Next, to address the potential impact of autocorrelation on tail index estimates, we applied autoregressive models of order p to the Garman-Klass range-based variances of each asset. The results indicate significant autocorrelation patterns in the processes generating range-based variances. The descriptive statistics indicates that even after accounting for higher-order autocorrelation, the innovation processes of the annualized daily range-based variances for all the assets display extremely heavy tails.

We then used the absolute values of the estimated innovation processes for each asset to estimate the power-law exponents. Notably, the estimated exponents closely align with those observed for the original data, providing strong evidence for the presence of genuine power-law behavior. Next, we performed Clauset *et al.*'s (2009) goodness-of-fit test, for the absolute values of the innovation processes of each asset. This procedure helps to evaluate whether the observed power-law behavior persists after accounting for autocorrelation, providing a robust check on the validity of the power-law estimates for our range-based variances. The goodness-of-fit test indeed indicated that the power-law null hypothesis holds for all innovation processes except gold, providing additional confirmation of the consistent power-law characteristics in the range-based variances. Additionally, the goodness-of-fit test results, with zero p-values across all cases, reject log-normal and exponential distributions, favoring the power-law distribution instead. These results support recent findings of Fathi *et al.* (2025) documenting that realized variances of Fama-French factors are subject to power-law behavior even after controlling for autocorrelations.

Finally, to validate the robustness of the power-law exponents, we performed sample-split tests by dividing the residual series for each asset into two equal-length subsamples. The consistency of tail exponents across both subsamples demonstrated that power-law behavior persists independently of sample-specific effects. Additionally, the goodness-of-fit test supports the power-law model in both subsamples for most assets, further enhancing the reliability of our findings.

A reader could be concerned about the robustness of tail estimation due to limited data in the extreme upper tail. However, the tail sample sizes in our study consistently exceed the empirical threshold suggested by Clauset *et al.* (2009), who argue that reliable estimation of power-law parameters typically requires a minimum of approximately 50 tail observations. For instance, in the case of Bitcoin, the number of observations in the power-law tail constitutes at least 3.41% of the total sample size of 3603—yielding more than 120 observations. Thus, the sample size in the tail comfortably meets the minimum requirement for credible tail exponent estimation using maximum likelihood techniques.

Another potential concern relates to whether our range-based volatility estimates sufficiently address market micro structure noise. In this regard, we note that our analysis is based on daily OHLC data and employs the Garman–Klass estimator, which has been identified as one of the most efficient and least noisy among range-based volatility measures (Molnár 2012). Importantly, microstructure noise is particularly problematic in high-frequency data, whereas range-based estimators constructed from daily prices are considerably less susceptible to such distortions. Thus, while no volatility estimator is entirely free from noise, the estimator we use represents a methodologically sound and practically robust choice that mitigates the typical concerns associated with market microstructure effects.

Finally, the potential influence of structural market features, such as liquidity and trading hours, on tail behavior merits attention. However, our results suggest that markets with widely varying characteristics—such as Bitcoin (traded 24/7 with relatively lower trading volume) and the S&P 500 (traded during regular hours with much higher volume)—exhibit statistically indistinguishable power-law exponents in range-based volatility. This finding is robust across asset classes, including commodities and FX. Additionally, trading volume in the S&P 500 has shown a clear upward trend over the sample period (see Figure A.2). As such, any attempt to split the sample into low- and high-liquidity regimes would effectively mirror our existing time-based splits (as in table 11), which already reveal stable tail exponent estimates

across subperiods. These observations suggest that structural differences such as trading hours and volume have limited impact on the tail behavior we observe.

7. Conclusion

This study presents novel evidence on the variance risk of financial markets by modeling range-based variances using the Garman-Klass variance estimator and analyzing their properties under hypothesized power-law distributions. Focusing on five key financial assets—S&P 500, gold, crude oil, the USD/GBP exchange rate, and Bitcoin—our findings reveal that range-based variances exhibit heavy tails, aligning closely with power-law distributions. These findings carry profound implications for financial modeling and risk management.

First, the estimated tail exponents for range-based variances consistently fall within the range $2 < \alpha < 3$, indicating characteristics of infinite variance-of-variance. As noted by Mandelbrot (1967), such variance can be considered 'so large that it may in practice be assumed infinite.' This challenges the foundational assumption of finite variances in traditional econometric models and highlights the limitations of statistical tools like *t*-tests, which are derived from the ordinary least squares (OLS) regression framework. The evidence of sample specificity, as highlighted by Fama's (1963) reflections on Mandelbrot's infinite variance hypothesis, underscores the inadequacy of moment-dependent statistical methods for handling the heavy-tailed distributions common in financial markets.

Second, goodness-of-fit tests consistently reject alternative distributions, including the widely used log-normal model, in favor of power-law distributions, emphasizing the inadequacy of conventional models in capturing the tail risks that define financial markets. Additionally, evidence derived from blocks bootstrap underscores the importance of accounting for dependency structures when estimating the standard deviations of tail exponents. Our joint test for a common power-law exponent reveals statistical invariance in power-law behavior for the range $(2.5 < q < 3.1)$ across all five assets, suggesting a universal factor governing variance risk. Autoregressive modeling of range-based variances further corroborates the persistence of power-law behavior even after adjusting for autocorrelation. Lastly, sample-split tests confirm the stability of power-law exponents over different time periods, reinforcing the robustness of the findings.

The empirical finding that a common power-law exponent governs realized variances across otherwise unrelated asset markets finds theoretical support in Gabaix (2016). In his comprehensive review, Gabaix (2016) outlines mechanisms—such as proportional random growth processes and universality—that explain why power-law distributions emerge across diverse economic systems. These mechanisms suggest that similar tail behaviors can arise in structurally different markets due to shared statistical properties, rather than asset-specific dynamics. Gabaix (2016) also emphasizes the concept of universality, where systems governed by different microfoundations may exhibit identical scaling laws at the macro level. This perspective aligns with the observation in our study that assets as diverse as crude oil, gold, and Bitcoin exhibit similar tail exponents. Furthermore, his discussion of aggregation effects and macroeconomic granularity provides a theoretical foundation for interpreting power-law regularities as emergent from complex but generalizable dynamics. Hence, our finding is consistent with and theoretically grounded in the framework developed by Gabaix (2016).

Furthermore, our results underscore the necessity of adopting alternative statistical frameworks for analyzing financial data and managing extreme risks. Effectively infinite variances and the rejection of log-normality suggests that reliance on traditional tools can significantly underestimate tail risks, particularly in environments characterized by extreme market events. The heavy-tailed nature of range-based variances has substantial implications for portfolio optimization, asset pricing, and risk management, necessitating frameworks that effectively account for the inherent extremity in financial data. By advancing a robust foundation for understanding variance risks across diverse asset classes, this study contributes to a more accurate and unified approach to financial modeling, particularly under infinite variance phenomena.

Despite its significant contributions, this study has limitations that merit consideration. For example, the analysis is limited to five financial assets—S&P 500, gold, crude oil, USD/GBP exchange rate, and Bitcoin—which constrains the generalizability of the findings to other asset classes or broader market conditions. Expanding the analysis to a wider range of assets and markets would enhance the applicability and breadth of the results.

8. Open Scholarship

This article has earned the Center for Open Science badge for Open Data. The data are openly accessible at (https://zenodo.org/records/15707465 (DOI 10.5281/zenodo.15707464).

Acknowledgments

The authors are grateful to the three anonymous referees for their valuable comments.

Data availability statement

The dataset has been deposited in Zenodo and is publicly available at: https://zenodo.org/records/15707465 (DOI 10.5281/zenodo.15707464).

Disclosure statement

No potential conflict of interest was reported by the author(s).

References

Andersen, T. G., Bollerslev, T., Diebold, F. X. and Ebens, H., The distribution of realized stock return volatility. *J. financ. econ.*, 2001, **61**(1), 43–76.

Andersen, T. G., Bollerslev, T., Diebold, F. X. and Labys, P., Modeling and forecasting realized volatility. *Econometrica*, 2001a, **71**(2), 579–625.

Andersen, T. G., Bollerslev, T., Diebold, F. X. and Labys, P., The distribution of realized exchange rate volatility. *J. Am. Stat. Assoc.*, 2001b, **96**(453), 42–55.

Andersen, T. G., Bollerslev, T. and Meddahi, N., Analytical evaluation of volatility forecasts. *Int. Econ. Rev. (Philadelphia)*, 2004, **45**, 1079–1110.

Andersen, T. G., Bollerslev, T., Diebold, F. X. and Labys, P., Modeling and forecasting realized volatility. *Econometrica*, 2003, **71**, 579–625.

Barndorff-Nielsen, O. E. and Shephard, N., Econometric analysis of realized volatility and its use in estimating stochastic volatility models. *J Roy Statist Soc Series B: Stat Method*, 2002, **64**(2), 253–280.

Barndorff-Nielsen, O. E. and Shephard, N., Power and bipower variation with stochastic volatility and jumps. *Journal of Financial Econometrics*, 2004, **2**(1), 1–37.

Bedowska-Sojka, B. and Kliber, A., Information content of liquidity and volatility measures. *Physica A*, 2021, **563**, 125436.

Bollerslev, T., Generalized autoregressive conditional heteroskedasticity. *J. Econom.*, 1986, **31**(3), 307–327.

Bollerslev, T. and Todorov, V., Tails, fears, and risk premia. *J Fin*, 2011, **66**(6), 2165–2211.

Bouchaud, J. P., Power laws in economics and finance: Some ideas fromphysics. *Quant Fin*, 2001, **1**(1), 105.

Bubák, V., Kočenda, E. and Žikeš, F., Volatility transmission in emerging European foreign exchange markets. *J Bank Fin*, 2011, **35**, 2829–2841.

Calvet, L. E. and Fisher, A. J., How to forecast long-run volatility: Regime switching and the estimation of multifractal processes. *J Fin Econom*, 2004, **2**(1), 49–83.

Chan, L. K. C., Karceski, J. and Lakonishok, J., New paradigm or same old hype in equity investing? *Fin Anal J*, 2000, **56**, 23–36.

Chou, R. Y., Chou, H. C. and Liu, N., Range volatility models and their application in finance. In *Handbook of Quantitative Finance and Risk Management*, edited by C. F. Lee, A. C. Lee and J. Lee, pp. 1273–1281, 2010 (Springer: Boston, MA).

Clauset, A., Shalizi, C. R. and Newman, M. E. J., Power-law distributions in empirical data. *SIAM Rev.*, 2009, **51**, 661–703.

Corsi, F., A simple approximate long-memory model of realized volatility. *J Fin Econ*, 2009, **7**(2), 174–196.

Creal, D., Koopman, S. J. and Lucas, A., Generalized autoregressive score models with applications. *J. Appl. Econ.*, 2013, **28**(5), 777–795.

Engle, R. F. and Rangel, J. G., The spline-GARCH model for low-frequency volatility and its global macroeconomic causes. *Rev Fin Stud*, 2008, **21**(3), 1187–1222.

Fama, E. F., Mandelbrot and the stable Paretian hypothesis. *J. Bus.*, 1963, **36**(4), 420–429.

Fama, E. F. and French, K. R., The cross-section of expected stock returns. *J Fin*, 1992, **47**, 427–465.

Fama, E. F. and French, K. R., Common factors in the returns on stocks and bonds. *J. Financ. Econ.*, 1993, **33**, 3–56.

Fama, E. F. and French, K. R., International tests of a five-factor asset pricing model. *J. Financ. Econ.*, 2017, **123**(3), 441–463.

Fama, E. F. and French, K. R., Choosing factors. *J. Financ. Econ.*, 2018, **128**(2), 234–252.

Fama, E. F. and French, K. R. The value premium. *Fama-Miller Working Paper No. 20–01*, 2020.

Fama, E. F. and French, K. R., A five-factor asset pricing model. *J. Financ. Econ.*, 2015, **116**, 1–22.

Fathi, M., Grobys, K. and Äijö, J., A common component of Fama and French factor variances. *Nor Am J Econ Fin*, 2025, **75**, 102292.

Fathi, M., Grobys, K. and Kolari, J. W., On the realized risk of foreign exchange rates: A fractal perspective. *J Risk Fin Manag*, 2024, **17**(2), 79.

Feng, G., Giglio, S. and Xiu, D., Taming the factor zoo: A test of new factors. *J Fin*, 2020, **75**, 1327–1370.

Gabaix, X., Power laws in economics: An introduction. *J Econ Pers*, 2016, **30**(1), 185–206.

Garman, M. B. and Klass, M. J., On the estimation of security price volatilities from historical data. *J. Bus.*, 1980, **53**(1), 67–78.

Gencay, R. and Selçuk, F., Extreme value theory and value-at-risk: relative performance in emerging markets. *Int. J. Forecast.*, 2004, **20**(2), 287–303.

Gençay, R., Selçuk, F. and Ulugülyağci, A., High volatility, thick tails and extreme value theory in value-at-risk estimation. *Ins: Mathe Econ*, 2003, **33**(2), 337–356.

Godfrey, L., *Bootstrap Tests for Regression Models*, 2009 (Palgrave Macmillan: Basingstoke).

Grigaityte, K. and Atwal, G. *Bayesian inference of power law distributions. bioRxiv*, 2019.

Grobys, K., What do we know about the second moment of financial markets? *Int Rev Fin Anal*, 2021, **78**, 101891.

Grobys, K., Correlation versus co-fractality: Evidence from foreign exchange rate variances. *Int Rev Fin Analy*, 2023, **86**, 102531.

Grobys, K., A universal exponent governing foreign exchange rate risks. *Int Rev Fin Anal*, 2024, **95**(Part B), 103422.

Hansen, B. E., Autoregressive conditional density estimation. *Int. Econ. Rev. (Philadelphia)*, 1994, **35**(3), 705–730.

Harvey, A. and Palumbo, D. Score-driven models for realized volatility. *Cambridge Working Papers in Economics*: 1950, 2019.

Hirshleifer, D., Investor psychology and asset pricing. *J Fin*, 2001, **56**, 1533–1597.

Lintner, J., The valuation of risk assets and the selection of risky investments in stock portfolios and capital budgets. *Rev. Econ. Stat.*, 1965, **47**(1), 13–37.

Lux, T. and Alfarano, S., Financial power-laws: Empirical evidence, models, and mechanisms. *Chaos, Solitons Fractals*, 2016, **88**, 3–18.

Mandelbrot, B., The variation of certain speculative prices. *J. Bus.*, 1963, **36**, 394–419.

Mandelbrot, B., The variation of some other speculative prices. *J. Bus.*, 1967, **40**, 393–413.

Mandelbrot, B. B., *The (Mis)behavior of Markets: A Fractal View of Risk, Ruin, and Reward*., 2008 (Profile Books).

Mandelbrot, B. B., Fisher, A. and Calvet, L. A multifractal model of asset returns. *Cowles Foundation Discussion Paper No.* 1164, 1997.

Markowitz, H., Portfolio selection. *J. Finance.*, 1952, **7**(1), 77–91.

Molnár, P., Properties of range-based volatility estimators. *Int Rev Fin Anal*, 2012, **23**, 20–29.

Mossin, J., Equilibrium in a capital asset market. *Econometrica*, 1966, **35**, 768–783.

Müller, U. A., Dacorogna, M. M., Davé, R. D., Olsen, R. B., Pictet, O. V. and Von Weizsäcker, J. E., Volatilities of different time resolutions—analyzing the dynamics of market components. *J Emp Fin*, 1997, **4**(2-3), 213–239.

Nelson, D. B., Conditional heteroskedasticity in asset returns: A new approach. *Econometrica*, 1991, **59**(2), 347–370.

Parkinson, M., The extreme value method for estimating the variance of the rate of return. *J. Bus.*, 1980, **53**(1), 61–65.

Renò, R. and Rizza, R., Is volatility lognormal? Evidence from Italian futures. *Physica A*, 2003, **322**, 620–628.

Schwert, G. W., Anomalies and market efficiency. In *Handbook of the Economics of Finance*, edited by G. M. Constantinides, M. Harris and R. M. Stulz, Vol. 1, pp. 939–974, 2003 (Elsevier Science B.V.: Amsterdam).

Shu, J. and Zhang, J. E., Testing range estimators of historical volatility. *J Fut Mark*, 2006, **26**, 297–313.

Sharpe, W. F., Capital Asset Prices: A Theory of Market Equilibrium under Conditions of Risk. *J. Finance.*, 1964, **19**(3), 425–442.

Shephard, N., *Stochastic Volatility: Selected Readings*, 2005 (Oxford University Press: Oxford).

Taleb, N. N., *Statistical Consequences of Fat Tails: Real World Preasymptotics, Epistemology, and Applications. Papers and Commentary*, 2020 (STEM Academic Press: New York).

Taylor, S. J., Financial returns modelled by the product of two stochastic processes—A study of daily sugar prices 1961–79. In *Time Series Analysis: Theory and Practice*, edited by O. D. Anderson, Vol. 1, pp. 203–226, 1982 (North-Holland).

Treynor, J. L. Toward a theory of market value of risky assets. Available at SSRN: https://ssrn.com/abstract=628187, 1962.

Virkar, Y. S. and Clauset, A., Power-law distributions and binned empirical data. *Ann. Appl. Stat.*, 2014, **8**(1), 89–119.

White, E., Enquist, B. and Green, J. L., On estimating the exponent of power-law frequency distributions. *Ecology*, 2008, **89**, 905–912.

Zakoian, J. M., Threshold heteroskedastic models. *J Econ Dyn Cont*, 1994, **18**(5), 931–955.

Zhang, L., Mykland, P. A. and Aït-Sahalia, Y., A tale of two time scales: Determining integrated volatility with noisy high-frequency data. *J. Am. Stat. Assoc.*, 2005, **100**(472), 1394–1411.

Appendix

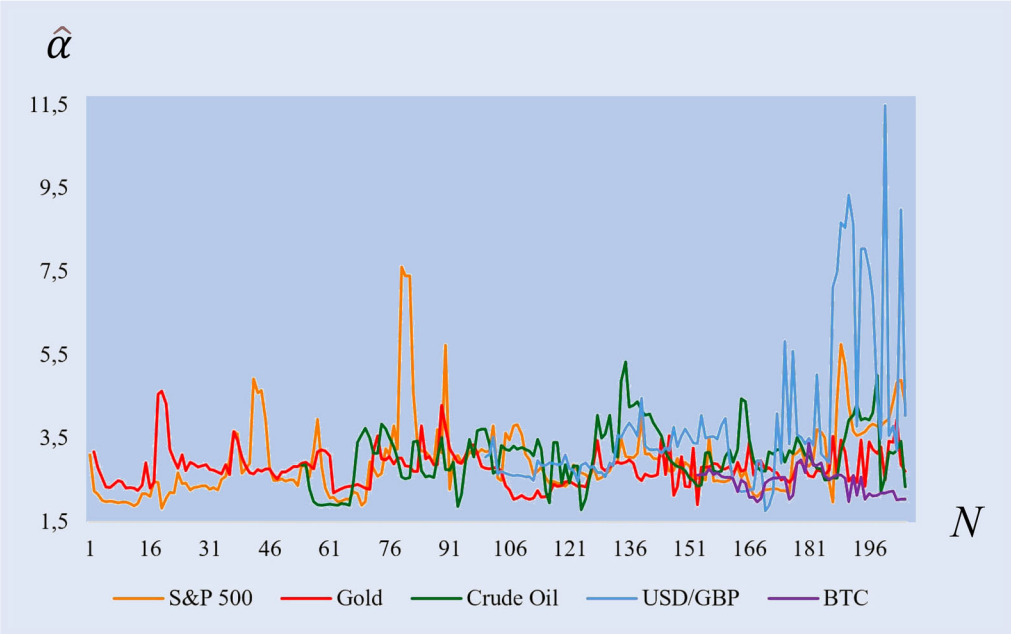

Figure A1. Time-varying estimated power-law exponents based on annualized daily range-based variances for various assets. Note: This figure plots the estimated power-law exponents derived from rolling window estimations based on annualized daily range-based variances for various assets, including the S&*P* 500, gold, crude oil, the USD/GBP exchange rate, and Bitcoin (BTC). The annualized daily range-based variances for each asset are calculated using the Garman-Klass methodology. The power-law exponents are estimated using the maximum likelihood estimation approach.

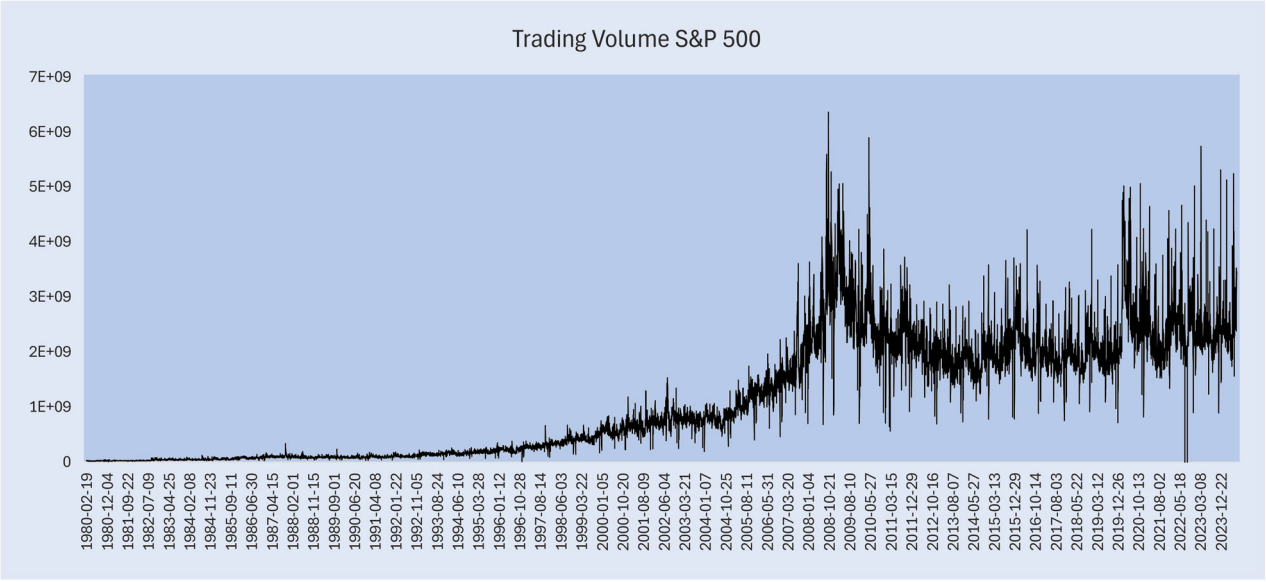

Figure A2. Trading volume of the S&*P* 500 over the sample period. Note: The figure displays the daily dollar trading volume over the sample period from February 19, 1980 to July 31, 2024.

Table A1. Descriptive statistics for weekly realized variance.

Statistic	S&*P* 500	Gold	Crude oil	USD/GBP	BTC
Mean	6.49	6.54	34.81	1.67	74.28
Median	2.99	3.35	15.36	1.09	35.46
Maximum	794.29	265.27	8330.27	78.36	4029.48
Minimum	0.02	0.02	0.14	0.01	0.00
Std. Dev.	22.28	12.33	220.41	3.01	189.70
Skewness	23.90	9.25	32.64	15.04	14.63
Kurtosis	758.30	142.91	1186.98	345.92	277.88
Observations	2242	2239	1711	1253	721
Period (MM/DD/YYYY)	02/19/1980	02/07/1980	01/02/1991	07/25/2000	09/17/2014
	07/31/2024	07/31/2024	07/31/2024	07/31/2024	07/31/2024

Note: This table presents the descriptive statistics of the weekly realized variance for various assets, including the S&*P* 500, gold, crude oil, USD/GBP exchange rate, and Bitcoin (BTC). The weekly realized variances for each asset calculated using the sum of the squared returns over five business days.

Table A2. Estimation of power-law exponents for weekly realized variance.

Metric	S&*P* 500	Gold	Crude oil	USD/GBP	BTC
$\hat{\alpha}$	2.51	2.24	2.43	2.84	2.93
$\hat{x}_{MIN}$	10.51	4.13	23.42	1.96	162.39
D	0.02	0.04	0.03	0.03	0.05
N_{PL}	12.53%	43.19%	33.26%	24.18%	10.40%
Std. Dev	0.09	0.04	0.06	0.11	0.22
Observations	2242	2239	1711	1253	721
Period (MM/DD/YYYY)	02/19/1980	02/07/1980	01/02/1991	07/25/2000	09/17/2014
	07/31/2024	07/31/2024	07/31/2024	07/31/2024	07/31/2024

Note: This table presents the estimation results for power-law exponents applied to the weekly realized variances of the S&*P* 500, gold, crude oil, the USD/GBP exchange rate, and Bitcoin. The weekly realized variances for each asset calculated using the sum of the squared returns over five business days. The parameter $\hat{\alpha}$ signifies the estimated tail exponent, while $\hat{\sigma}$ denotes the estimated standard deviation. The lower threshold $\hat{x}_{MIN}$ is identified through the optimized Kolmogorov-Smirnov distance (D), following the procedure described by Clauset *et al*. (2009). The reported $\hat{x}_{MIN}$ corresponds to the optimal distance D. Additionally, the fraction of observations obtained by the power-law process, denoted as N_{PL} is provided for each asset.

Table A3. Goodness-of-fit tests for the weekly realized variance.

Asset market	Power-law	Log-normal	Exponential
S&*P* 500	0.99	0.58	0.00
Gold	0.04	0.65	0.00
Crude oil	0.34	0.11	0.00
USD/GBP	0.67	0.31	0.00
BTC	0.73	0.31	0.00

Note: This table presents the results (viz., p-values) of the goodness-of-fit tests for weekly realized variance, conducted using the Kolmogorov-Smirnov (KS) method to assess whether the empirical data and the synthetic data—generated from a power-law distribution specified by x_{min} and α —originate from the same underlying distribution (column 2). Additionally, the table includes the results of goodness-of-fit tests for log-normal and exponential distributions in columns 3 and 4, respectively. The null hypothesis for these tests states that the empirical data and the synthetic data generated from the specified distributions (log-normal and exponential) are consistent, suggesting that each distribution provides an acceptable fit to the observed data. The weekly realized variances for each asset market are calculated using the sum of the squared returns over five business days.

Table A4. Descriptive statistics of estimated power-law exponents derived from rolling window estimations.

Statistic	S&*P* 500	Gold	Crude Oil	USD/GBP	BTC
Minimum	1.83	1.91	1.79	1.76	1.98
5% Qnt.	1.99	2.17	1.92	2.28	2.04
10% Qnt.	2.10	2.31	2.22	2.54	2.05
Median	2.73	2.77	3.11	3.24	2.54
90% Qnt.	3.88	3.34	4.04	7.01	2.84
95% Qnt.	4.59	3.55	4.27	8.41	2.91
Maximum	7.61	4.63	5.33	11.48	3.38
Mean	2.96	2.79	3.09	3.78	2.45
Std. Dev	0.92	0.44	0.68	1.82	0.31
Excess Kurtosis	7.48	2.67	0.32	4.19	− 0.06
Skewness	2.26	1.15	0.39	2.17	0.35
N	205	204	152	106	53

Note: This table reports descriptive statistics for estimated power-law exponents derived from rolling window estimations based on annualized daily range-based variances for various assets, including the S&*P* 500, gold, crude oil, the USD/GBP exchange rate, and Bitcoin (BTC). The annualized daily range-based variances for each asset are calculated using the Garman-Klass methodology. The power-law exponents are estimated using the maximum likelihood estimation approach. Quintiles (Qnt) are reported from the 5th to the 95th percentile.

Table A5. Important subfamilies of the GB2 distribution.

Subfamily	Condition
Generalized Gamma	$q \to \infty$
Beta Prime	$a = 1$
F-distribution	$a = 1, b = 1, p = \frac{d_1}{2}, q = \frac{d_2}{2}$
Singh–Maddala	$p = 1$
Dagum distribution	$q = 1$
Pareto type IV	$p = 1, b = 1$

Note: The Generalized Beta of the Second Kind (GB2) is a four-parameter family of continuous probability distributions that encompasses a wide variety of shapes. The GB2 distribution is defined as:

$$f(x;a;b;p;q) = \frac{a(x/b)^{ap-1}}{bB(p,q)[1+(x/b)^a]^{p+q}},$$

where $B(p,q)$ is the Beta function, $a > 0$ is the tail parameter controlling the tail heaviness, $b > 0$ is a scale parameter, $p > 0$, $q > 0$ are shape parameters that also govern skewness. This table reports important subfamilies of the GB2 distribution.

Table A6. Estimated parameters of the GB2 distribution.

Range-based variance	a	b	p	q
S&*P* 500	125.30	4.44	67.73	0.016
Gold	114.95	6.36	116.26	0.015
Crude oil	73.95	22.47	113.15	0.022
USD/GBP	108.31	1.05	105.28	0.016
BTC	223.86	243.08	0.0255	0.0094

Note: The Generalized Beta of the Second Kind (GB2) is a four-parameter family of continuous probability distributions that encompasses a wide variety of shapes. The GB2 distribution is defined as:

$$f(x;a;b;p;q) = \frac{a(x/b)^{ap-1}}{bB(p,q)[1+(x/b)^a]^{p+q}},$$

where $B(p,q)$ is the Beta function, $a > 0$ is the tail parameter controlling the tail heaviness, $b > 0$ is a scale parameter, $p > 0$, $q > 0$ are shape parameters that influence the distribution's form, including its skewness. This table reports the parameter estimates for GB2 distributions fitted to the data ranges defined by the power-law cutoffs listed in table 3.